REVIEWS

Hydrogel ionotronics

Canhui Yang and Zhigang Suo *

Abstract | An ionotronic device functions by a hybrid circuit of mobile ions and mobile electrons. Hydrogels are stretchable, transparent, ionic conductors that can transmit electrical signals of high frequency over long distance, enabling ionotronic devices such as artificial muscles, skins and axons. Moreover, ionotronic luminescent devices, ionotronic liquid crystal devices, touchpads, triboelectric generators, artificial eels and gel–elastomer–oil devices can be designed based on hydrogels. In this Review, we discuss first-generation hydrogel ionotronic devices and the challenges associated with the mechanical properties and the chemistry of the materials. We examine how strong and stretchable adhesion between hydrophilic and hydrophobic polymer networks can be achieved, how water can be retained in hydrogels and how to design hydrogels that resist fatigue under cyclic loads. Finally, we highlight applications of hydrogel ionotronic devices and discuss the future of the field.

Living matter conducts electricity mostly using ions, while machines conduct electricity mostly using electrons. The two systems, natural and synthetic, function through distinct ionic and electronic circuits; however, ionic and electronic circuits are coupled at human–machine interfaces in the electrophysiological study of the brain, heart and muscle[1–6] (FIG. 1a). Hybrid circuits of ions and electrons also enable batteries[7,8], supercapacitors[9,10] and fuel cells[11,12]. Human–machine interfaces and energy-storage devices have inspired the field of ionotronics (also called iontronics), in which devices function by using both mobile ions and electrons[13–16].

In this Review, we discuss ionotronic devices that use hydrogels as stretchable, transparent ionic conductors. Hydrogels are an integral part of living matter; many tissues and organs of animals and plants are hydrogels. A hydrogel contains a polymer network and water molecules (FIG. 1b). The polymer network makes the hydrogel an elastic solid, and the water molecules make the hydrogel an ionic conductor. The polymer network has a mesh size of ~10 nm, which is much larger than the size of a water molecule, allowing water molecules in the hydrogel to maintain the same chemical and physical properties as in liquid water. Dissolving salt in water yields mobile ions, which change the resistivity of the water from ~18.2 MΩm (the value of purified water) to ~10^{-1} Ωm, depending on the type and concentration of the salt[17]. Mobile ions and electrons form an electric double layer (EDL) at the interface between a hydrogel and a metal (FIG. 1c). The EDL functions as a capacitor with a capacitance of ~10^{-1} F m^{-2} and couples the ionic current in the hydrogel and the electronic current in the metal.

Hydrogel ionotronics rely mostly on non-Faradaic processes, with no matter or charge crossing the interface. The hydrogel can be connected to an ionic device or a living tissue, and the metal can be connected to an electronic device. At first approximation, the electrochemistry of hydrogels is similar to that of aqueous electrolytes, which has been extensively studied[18]; however, aqueous electrolytes are liquids, and hydrogels are solids, allowing a broad range of applications. For example, hydrogels have long been used in electrophysiological measurements to connect metallic electrodes and living tissues[19,20]. A hydrogel can be stretched several times its initial length and recover elastically, with its elastic moduli being readily tuned from 1 kPa to 100 kPa, or even beyond this range. The elasticity is entropic and results from the change in the configuration of the polymer network and water molecules, negligibly affecting the ionic conductivity. Thus, stretching a strip of hydrogel λ times its initial length leads to a change in resistance by a factor of approximately λ^2 (FIG. 1d). The polymer network does not scatter light, which makes the hydrogel highly transparent to visible light of all colours, similar to the optical properties of water. A hydrogel retains transparency as the thickness increases and the resistance decreases (FIG. 1e). This combination of properties makes hydrogels ideal materials for ionotronic devices, including artificial muscles[21–28], artificial skins[29–33], artificial axons[13], ionotronic luminescent devices[34,35], ionotronic liquid crystal devices[36], touchpads[37], triboelectric generators[38–40], artificial eels[41] and gel–elastomer–oil (GEO) devices[42–44], for applications such as wearable electronics for humans and robots and implantable human–machine interfaces.

Compared with synthetic materials such as metals, ceramics, plastics and semiconductors, synthetic

John A. Paulson School of Engineering and Applied Sciences, Kavli Institute for Bionano Science and Technology, Harvard University, Cambridge, MA, USA.

**e-mail: suo@seas.harvard.edu*

https://doi.org/10.1038/s41578-018-0018-7

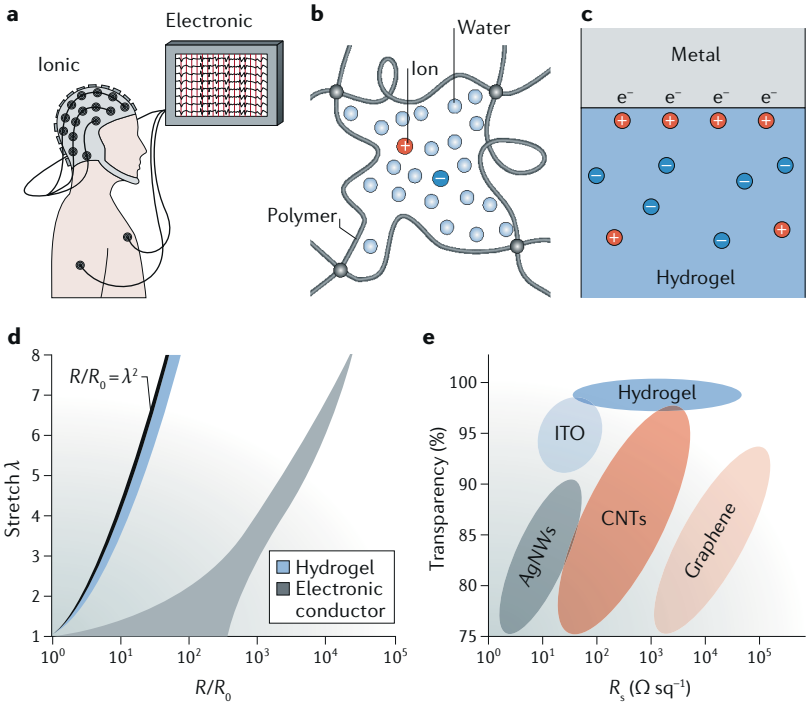

Fig. 1 | **Hydrogels as ionic conductors. a** | Measuring the electrophysiology of the brain, heart and muscle requires mobile ions and mobile electrons. **b** | Hydrogels are made of polymer networks, which make a hydrogel an elastic solid, and water, which makes the hydrogel an ionic conductor. **c** | At the interface between a hydrogel and a metal, mobile ions in the hydrogel and mobile electrons in the metal form an electric double layer. **d** | An electronic conductor breaks at a smaller stretch, λ, than a hydrogel. **e** | Electronic conductors are less transparent at low resistance, R_s, than hydrogels. AgNWs, silver nanowires; CNTs, carbon nanotubes; ITO, indium tin oxide; R, electrical resistance in the stretched state; R_0, electrical resistance in the initial state. Panels **d** and **e** are adapted with permission from REF.[21], AAAS.

hydrogels, first reported for biological use in the 1960s[45], are relatively new but rapidly evolving materials for biomedical applications, for example, in contact lenses[46], superabsorbent diapers[47], cell cultures[48], tissue regeneration[49] and drug delivery[50]. In these applications, synthetic hydrogels mimic the optical, mechanical and chemical functions of living tissues but not their electrical functions or properties. The field of hydrogel ionotronics has benefited from biological applications of synthetic hydrogels but also faces previously unmet challenges.

In this Review, we discuss first-generation hydrogel ionotronic devices. We highlight areas of materials research that are directly motivated by hydrogel ionotronics, including the engineering of strong and stretchable adhesion between hydrophilic and hydrophobic polymer networks[51–53], the retention of water in hydrogels in air[29,51,54,55] and the improvement of fatigue resistance in hydrogels under cyclic loads[56–67]. We provide an overview of all hydrogel ionotronic devices that have been described in the literature so far, with an emphasis on the fundamental principles of hydrogel ionotronics and challenges regarding the mechanical properties and chemistry of the materials. Finally, immediate opportunities in the field of hydrogel ionotronics are highlighted.

Artificial muscle, skin and axon

First-generation hydrogel ionotronic devices have been explored to mimic neuromuscular and neurosensory systems. Ionic signals play a key role in neurosensing; for example, stepping on a nail results in an ionic signal triggered by the contact between the metal and the skin[68]. The ionic signal propagates along the axon to the central nervous system, which, in response, generates an ionic signal and sends it in two directions: to the brain to register the pain and to the muscle to lift the foot. Hydrogel ionotronic devices mimic the functions but not the anatomies of the skin, axon and muscle. The nervous system senses, decides and acts through a combination of ionic signalling and chemistry; however, the hydrogel ionotronic device applies a combination of ionics and electronics.

Artificial muscle

Muscles convert chemical reactions into mechanical movements. Pelrine and co-workers invented the first artificial muscles that convert electric voltages into mechanical movements[69,70]. These artificial muscles, called dielectric elastomer actuators, have undergone substantial development, enabling a broad range of applications, including soft robots, prosthetic devices and adaptive optics[69,71–74].

An ionotronic artificial muscle comprises a layer of elastomer sandwiched between two layers of hydrogel[21] (FIG. 2a). The elastomer is a dielectric, the hydrogel is a conductor and the sandwich is a capacitor. Metallic wires connect the two hydrogel layers to an external power source. Voltage applied between the two metallic wires by the power source leads to the movement of mobile electrons in the metals and mobile ions in the hydrogels either away from or towards the interfaces between the metals and the hydrogels. At the same time, mobile ions accumulate at the two interfaces between the hydrogels and the elastomer. The two hydrogel–elastomer interfaces are charged with opposite polarities, and their attraction causes a decrease in the thickness and an increase in the area of the elastomer. The hydrogels can be made much softer than the elastomer, so that the hydrogels do not restrict the deformation of the elastomer. The electromechanical coupling is highly nonlinear and, depending on the geometry, enables different designs of artificial muscles and many modes of electromechanical instability[72–76]. Both the elastomer and hydrogel can be made transparent, and the metal wires can contact the hydrogels in regions outside of the active area, making the whole ionotronic artificial muscle transparent (FIG. 2a).

The voltage needed to considerably deform the elastomer scales as $V \approx H_E(\mu_E/\varepsilon_E)^{1/2}$, in which V is the voltage applied across the thickness of the elastomer and H_E, μ_E and ε_E are the thickness, shear modulus and permittivity of the elastomer, respectively[75]. The electric field in the elastomer scales as $E \approx (\mu_E/\varepsilon_E)^{1/2}$. Representative values of such ionotronic artificial muscles are $H_E = 10^{-4}$ m, $\mu_E = 10^5$ Pa and $\varepsilon_E = 10^{-11}$ F m^{-1}, with a voltage of $V \approx 10^4$ V and an electric field of $E \approx 10^8$ V m^{-1}. The artificial muscle operates at high voltage but with low current. Careful design can mitigate concerns regarding

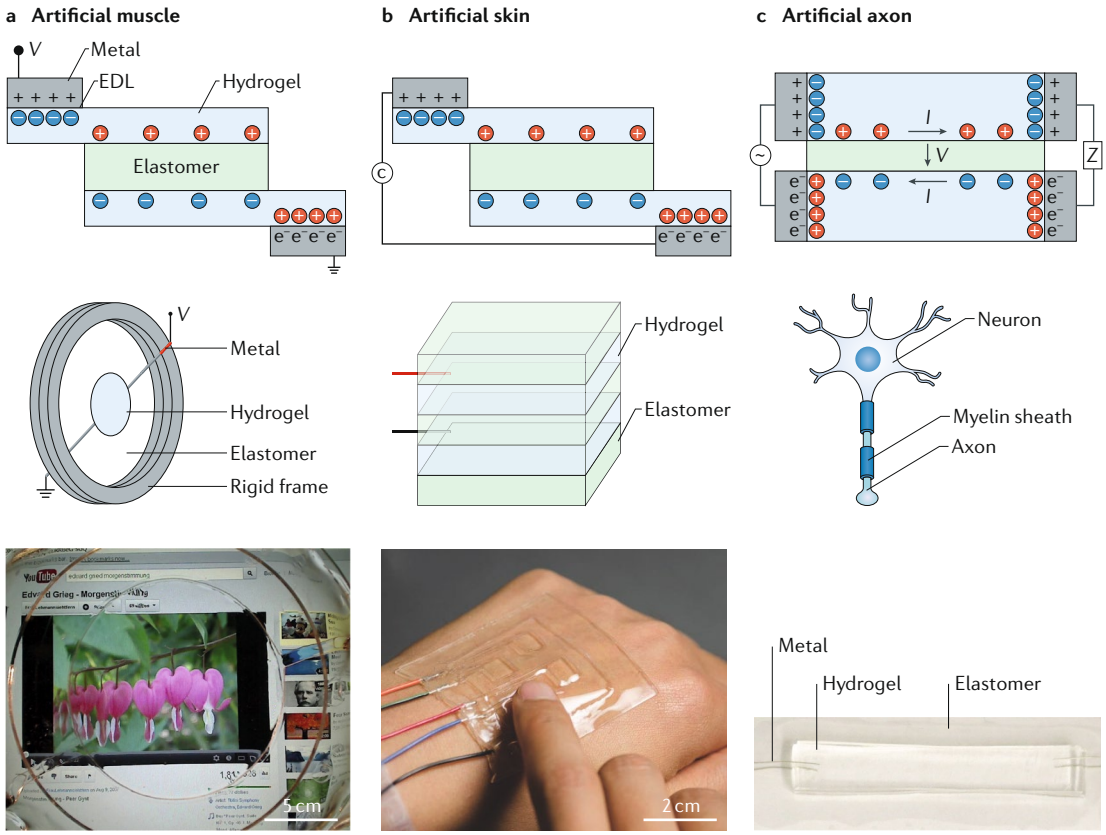

Fig. 2 | **Artificial muscle, skin and axon. a** | An artificial muscle consists of an elastomer sandwiched between two hydrogels, connected to a source of electrical power by metallic wires. The interface between the metal and the hydrogel forms an electrical double layer (EDL). If a voltage, *V*, is applied between the two metal wires, the hydrogels conduct ions, and mobile ions of opposite polarities accumulate at the interfaces between the hydrogel and elastomer, causing a decrease in the thickness and an increase in the area of the elastomer. To realize an artificial muscle, a sheet of elastomer is radially pre-stretched and fixed to a circular rigid frame. In the centre of the elastomer, thin layers of hydrogels are attached to both sides of the elastomer. Each layer of hydrogel is connected to a metallic electrode. For example, a hydrogel ionotronic loudspeaker is transparent and plays music (ionic music or iTunes). **b** | An artificial skin consists of an elastomer sandwiched between two hydrogels, connected to a capacitor meter, c, by two metallic wires. Pressure or stretching causes the elastomer to change shape and capacitance. An array of such pressure sensors (ionic skin, iTouch or iPad) can be attached to the back of a hand. **c** | In an artificial axon (ionic cable), two hydrogel layers are insulated by a layer of elastomer. The input port connects to a source of time-varying voltage, *V*, and the output port connects to a load of impedance, *Z*. In a myelinated axon, the myelin sheath is a dielectric, and body fluid is the electrolyte. *I*, ionic current. Panel **a** is adapted with permission from REF.[21], AAAS. Panel **b** is adapted with permission from REF.[29], John Wiley and Sons. Panel **c** is adapted with permission from REF.[13], Elsevier.

safety. For example, an ionotronic fish can be designed to swim in water and to be held in the hand[25]. The operating voltage can further be reduced by decreasing the thickness or elastic modulus or by increasing the permittivity of the elastomer[77,78].

The high operating electric field of artificial muscles requires elastomers of high electric breakdown strength. In their pioneering work, Pelrine and co-workers demonstrated that the acrylic elastomer[69] VHB manufactured by 3 M Inc. attains an electric breakdown strength of ~4×10^8 V m^{-1}, comparable to that of thin films of silicon dioxide (~10^9 V m^{-1}), which are commonly used in microelectronics. VHB is highly transparent and stretchable and has since been widely used for the design of artificial muscles; however, the time-dependent stress–stretch behaviour of VHB is not ideal for many applications[69,71–74]. Artificial muscles require elastomers that possess high electric breakdown strength, high permittivity and low hysteresis. Different elastomer chemistries are being explored[74,78–83], but the lack of a clear figure of merit has complicated the development of the ideal elastomer for artificial muscles. In particular, little is known about the long-term stability of hydrogel–elastomer laminates subjected to high voltage[21].

Many existing dielectric elastomer devices use carbon grease instead of hydrogels as compliant electrodes[69,84,85]. Carbon grease is a plastic liquid, like toothpaste. Plastic liquids do not flow if the applied stress is below the yield strength of the material but do flow if the applied stress is above the yield strength. The plasticity of carbon grease provides the rheological requirements for artificial muscle devices. Carbon grease can be brushed onto the surface of the elastomer, and on a stationary elastomer, the carbon grease remains stationary and does not drip under gravity or small disturbances. The carbon

grease also conforms to an elastomer undergoing large and repeated elastic deformation. However, it can form wave-like patterns if the elastomer is subjected to large deformations over many cycles[86,87], and it is sticky and opaque. Therefore, other stretchable conductors have been developed for artificial muscles, such as carbon nanotubes, graphene, patterned metal electrodes, metallic nanoclusters, metallic nanowires and conducting polymers[85,88]. All these electronic conductors are stretchable, but it remains a challenge to make them transparent at the same time. Aqueous electrolytes have also been used as conductors in artificial muscles, but in liquid form[89–91]. By contrast, hydrogels are used in solid form and have the advantage of providing a stretchable and transparent polymer network as conductors.

The high voltage required to operate an ionotronic artificial muscle raises the question[21] of whether the EDL between a hydrogel and a metal averts an electrochemical reaction. Certain electrode–electrolyte interfaces are non-Faradaic, that is, they do not react as long as the voltage across the interfaces is sufficiently small (≤1 V)[92]. In series with the elastomer, the EDL behaves like an additional capacitor (FIG. 2a). At the EDL, charges of opposite polarities separate at the nanometre scale, endowing the EDL with a capacitance per unit area of $c_{EDL} \approx 10^{-1}$ F m^{-2} (REF.[93]). By contrast, the elastomer separates charges of opposite polarities at the millimetre scale and thus has a much smaller capacitance per unit area of $c_E \approx 10^{-8}$ F m^{-2}. Charge balance requires that $c_{EDL}A_{EDL}V_{EDL} = c_EA_EV_E$, in which A_{EDL} and A_E are the areas of the EDL and elastomer, respectively, and V_{EDL} and V_E are the voltages across the EDL and elastomer, respectively. For $A_{EDL}:A_E > 10^{-4}$, the voltage across the EDL is small, $V_{EDL} < 1$ V, owing to the large capacitance ratio, $c_{EDL}:c_E \approx 10^7$, even if the voltage across the elastomer, V_E, is on the order of 1 kV. Hydrogels contact the metals outside the active area of the device, and therefore, the criterion of $A_{EDL}:A_E > 10^{-4}$ is easy to fulfil. If necessary, the area of the EDL can be increased using porous electrodes similar to those used in supercapacitors.

Another important consideration is whether a hydrogel transmits an electrical signal fast enough[21]. A hydrogel has high resistivity, $\rho \approx 10^{-2}$ Ωm, which is about a million times higher than that of copper. However, ionic conduction ensures fast signal transduction, for example, humans can move their limbs within milliseconds after a thought has formed in the brain. The fast signal transduction of hydrogels through ionic conductivity has initially inspired the development of hydrogel ionotronics. The elastomer endows the artificial muscle with capacitance, and resistance is provided by the hydrogels. For a working area of $A_E \approx 10^{-2}$ m^2 and with a hydrogel resistance of $R \approx 100$ Ω, the resistive–capacitive (RC) delay of the artificial muscle is estimated to be 10^{-8} s. This RC delay is much smaller than the period of the drive voltage or the fundamental resonance owing to the elasticity and inertia of the artificial muscle[21]. Thus, a hydrogel transmits electrical signals fast enough to enable the operation of an ionotronic artificial muscle. The introduction of hydrogels as stretchable and transparent electrodes has broadened the scope of applications for dielectric elastomer actuators, for example, for transparent loudspeakers[21], artificial fish[25] and soft robots[42,43].

Artificial skin

Human skin is a stretchable, large-area sheet of distributed sensors of pressure, deformation, temperature and humidity. These characteristics have inspired the development of artificial skins to enable wearable or implantable electronics for entertainment and health care[2,94–97] by using stretchable electronic conductors or stretchable ionic conductors such as hydrogels. A hydrogel-based ionotronic artificial skin comprises an elastomer sandwiched between two hydrogels[29] (FIG. 2b). The two hydrogels connect to a capacitive meter through two metallic wires. The artificial skin is usually encapsulated by two additional layers of elastomer for electrical insulation and water retention. Both the elastomer and hydrogel are transparent and stretchable, and the metallic wires are outside of the active area, making the ionotronic artificial skin transparent and stretchable[29] (FIG. 2b).

The contacts between the hydrogels and the metallic wires form two EDL capacitors in series with the elastomer capacitor. The capacitance of the EDL is much larger than that of the elastomer, and therefore, the equivalent capacitance is dominated by the elastomer capacitance, $\varepsilon_E A_E/H_E$, in which ε_E, A_E and H_E are the permittivity, area and thickness of the elastomer, respectively. If pressure is applied or the elastomer is stretched, the thickness of the elastomer is decreased, and the area is increased. The change in shape causes a change in capacitance, which is recorded by the capacitive meter. Unlike the artificial muscle that deforms in response to high voltage, the artificial skin deforms in response to applied forces, and the corresponding change in capacitance can be measured at voltages ≤1 V. The hydrogel ionotronic artificial skin can sense single touch events while remaining functional in the deformed state[29], can sense multiple touches[30] and can self-heal[31,33].

Ionotronic artificial skins have also been designed to sense changes in resistance[98,99]. Current hydrogel ionotronic artificial skins sense only pressure and deformation; however, hydrogels can also be used to convert changes in temperature and humidity into electrical signals, mimicking the function of human skin.

Artificial axon

Axons transmit ionic signals to coordinate sensing, decision-making and function. An artificial axon mimics the function of an axon and certain aspects of its anatomy. In an ionotronic artificial axon, two hydrogel layers are separated by a layer of elastomer[13] (FIG. 2c), inspired by the structure of a myelinated axon[68], which features a saline solution as the electrolyte and myelin, which is the fatty sheath of the axon, as the dielectric shell. The electrolyte and the dielectric shell establish a fast conduit for electrical signals. In the artificial axon, the dielectric elastomer mimics the myelin sheath, and the electrolytic hydrogel mimics body fluid. One end of the artificial axon serves as the input port and connects to an external power source, and the other end serves as the output port and connects to a load Z. If a time-dependent signal is applied, the artificial axon can transmit the signal from the input port to the output port.

In an artificial axon, the contacts between hydrogels and metallic wires form four EDLs. The artificial axon can transmit alternating voltage only at an amplitude ≤1 V across the EDL to function without electrolyzing the EDLs. The voltage between the top and bottom hydrogels is described by $v(x,t)$, in which x is the location along the length of the artificial axon and t is the time. The voltage obeys the diffusion equation, $\partial v/\partial t = D\,\partial^2 v/\partial x^2$, in which D is the diffusivity of the electrical signal. In a layered cable design, the diffusivity of an electrical signal scales as $D \approx ab/(\rho\varepsilon_E)$, in which a and b are the thicknesses of the hydrogel and the elastomer, respectively, ρ is the resistivity of the hydrogel and ε_E is the permittivity of the elastomer[13]. Using the representative values $a = b = 10^{-3}$ m, $\rho = 10^{-2}$ Ωm and $\varepsilon_E = 10^{-11}$ F m^{-1}, the diffusivity of an electrical signal in the artificial axon can be calculated as $D \approx 10^7$ m^2 s^{-1} (REF.[13]). This diffusivity is many orders of magnitude larger than that of ions in water ($D_{ion} \approx 10^{-9}$ m^2 s^{-1})[100]. Thus, transmitting an ionic signal along the artificial axon does not require ions to migrate from one end to the other. Rather, ions just need to move locally to enable propagation of the electric field.

The high diffusivity of the signal allows the artificial axon to transmit signals over a long distance and at high frequency, but it does not invoke depolarization. By contrast, a human axon transmits an action potential without decay in amplitude by continuously depolarizing its membrane[101]. However, because the voltage obeys the diffusion equation, the signal will not significantly decay if the length of the artificial axon is smaller than the diffusion length, $\omega\rho\varepsilon_E L^2/(ab) \ll 1$, in which ω is the angular frequency of the signal and L is the length of the artificial axon. A signal with a frequency of 1 MHz can be readily transmitted along a 1 m long artificial axon[13]. The scaling relation further indicates that the artificial axon does not change its behaviour if the length and the thickness of the hydrogel and the elastomer are proportionally decreased, enabling the miniaturization of ionic circuits.

The artificial axon can transmit power to resistors, capacitors, inductors and semiconductor components. Light-emitting diodes function only if electrons flow in one direction; however, an artificial axon can light up diodes without electrolysis through a 'rocking-chair' design, which connects two diodes with antiparallel polarity[13]. The EDLs do not allow continuous electron flow, but the rocking-chair design enables the two diodes to inject electrons to each other, illustrating the possibility to design ionotronic circuits that involve both hydrogels and semiconductor components.

The use of hydrogels further makes artificial axons highly stretchable and transparent[13] (FIG. 2c), with the axon remaining functional despite being stretched several times its original length. These properties make artificial axons applicable as interconnects for wearable and implantable devices and for soft robots[99,102].

Hydrogel ionotronic devices

Optoelectronic devices

Optoelectronic devices often require materials that combine optical transparency and electrical conductivity. The widely used transparent electrode, indium tin oxide (ITO), is rigid, brittle and costly, hampering the use of optoelectronic devices for mobile and wearable applications. Therefore, stretchable and transparent electronic conductors are being developed using soft matrices that contain conducting materials, such as patterned wires[103,104], conducting polymers[105,106], carbon nanotubes[107,108] and silver nanowires[109,110]. However, these conductors are limited by low stretchability[88], low transparency[111] and degradation under cyclic loading[112].

By contrast, hydrogels achieve high transparency and stretchability without sacrificing conductivity (FIG. 1d,e). Hydrogels can contain ions at multiple moles per litre, gaining a resistivity of ~10^{-1} Ωm (REF.[54]), which is much higher than that of ITO (~10^{-5} Ωm); however, a millimetre-thick hydrogel can achieve a surface resistance of 100 Ω sq^{-1} and still retain an optical transparency of 99.9%[21]. The softness of hydrogels further enables large and elastic deformation over many deformation cycles[21,56–58], and hydrogels maintain conductivity even when highly stretched[21]. The properties of a hydrogel can be tuned by modifying its components[113–115], allowing for the design of tough hydrogels similar to natural rubber[116,117] and of hydrogels that retain water in low-humidity environments[54]. These properties make hydrogels ideal candidates as electrodes in electro-optical devices, providing both electro-optical performance and high stretchability.

Ionotronic luminescence. Phosphors have long been used in displays and for solid-state lighting[118]. Phosphors emit light in response to an electric current or an alternating electric field. In the latter case, the alternating electric field generates mobile electrons and holes from the interior of the phosphors, which subsequently recombine to produce light. The mobile electrons and holes are not injected into the phosphors from an external power source. Therefore, an electronic conductor can be replaced with an ionic conductor in electroluminescent devices[34,35].

An ionotronic luminescent device consists of a layer of phosphor particles sandwiched between two elastomer layers and two hydrogel layers[34,35] (FIG. 3a). An applied alternating voltage causes ions of opposite polarities to produce an electric field, lightening up the phosphor. The hydrogels and elastomers are transparent, allowing light to be transmitted. The metallic wires are in contact with the hydrogels to connect the device to an external power source located outside of the luminescing area to avoid blocking the light. The use of hydrogels and elastomers makes the device stretchable, and stretchability is not compromised by the brittle phosphor particles owing to their small size (ranging in diameter from nanometres to tens of micrometres) (FIG. 3b,c).

Conventional electroluminescent devices operate at a voltage of ~10 V (REF.[118]). By contrast, hydrogel ionotronic luminescent devices operate at voltages ranging from 100 V to 10 kV (REFS[34,35]), which can be decreased to allow applications for wearable applications. When the phosphor luminesces, the EDLs between the hydrogels and metals do not undergo electrolysis, and the elastomer does not undergo electric breakdown. The three types of capacitors — the EDL, the elastomer and the phosphor — are in series. The EDLs only sustain voltages of <1 V

if $A_{EDL}:A_E > 10^{-4}$. For the elastomer and the phosphor, the balance of electric charge requires that $\varepsilon_E E_E = \varepsilon_p E_p$, in which ε_E and E_E are the permittivity and the electric field in the elastomer, respectively, and ε_p and E_p are the corresponding quantities in the phosphor. Typically, the permittivity of the elastomer and phosphors are of the same order of magnitude. For example, the permittivity of zinc sulfide, a widely used and commercialized phosphor, is $\varepsilon_p \approx 8.5$ (REF.[119]), and the permittivity of VHB is $\varepsilon_E \approx 4.7$ (REF.[24]). The electric field enabling luminescence of the phosphors is one order of magnitude lower than the electric breakdown strength of the elastomer. For example, zinc sulfide luminesces under an electric field of $E_p \approx 10\,V\,\mu m^{-1}$ (REF.[118]), and the electric breakdown strength of VHB is $\geq 100\,V\,\mu m^{-1}$ (REF.[24]). Therefore, the elastomer does not suffer electric breakdown when the phosphor luminesces. The high voltage in hydrogel ionotronic luminescent devices is required because of the thickness (~1 mm) of the elastomer. Decreasing the dielectric elastomer thickness, for example, to 1 μm, allows for a decrease in the working voltage to 10 V. Moreover, the *RC* delay of hydrogel ionotronic luminescent devices is $\sim 10^{-8}$ s, similar to that of an artificial muscle, and thus does not limit the response speed because the working frequency of electroluminescent devices usually ranges from 10^2–10^4 Hz (REF.[118]).

The elastomer has several functions in hydrogel ionotronic luminescent devices. It prevents the device from electric breakdown, it separates the two hydrogel layers and it isolates the phosphors from the hydrogel and the environment. The long-term stability of ionotronic luminescent devices has not yet been systematically studied, but phosphors are known to degrade at high humidity[120]. However, we have developed elastomer-encapsulated devices that remain functional for more than 8 months despite being stored at ambient conditions[34]. Moreover, stable phosphors are currently being developed[121,122].

Ionotronic luminesce can operate over large areas. Electric charge balance requires that $c_{EDL}A_{EDL}V_{EDL} = c_pA_pV_p$, in which c_p, A_p and V_p are the capacitance per unit area, the area and the voltage across the phosphor, respectively. Using representative values, an area of $A_p < 10^2 A_{EDL}$ is obtained. Thus, the device can stably operate without electrolyzing the EDL if the working area is <100 times the area of the EDL. The EDLs are located outside of the working area, and therefore, it is easy to scale up the EDL area, for example, by using porous electrodes; for an EDL area of $A_{EDL} = 1\,m^2$, the maximum working area is $100\,m^2$.

The softness and stretchability of ionotronic luminescent devices provide opportunities for applications in soft robotics and wearable electronics. For example, the geometry of ionotronic luminescent devices resembles that of a capacitive pressure sensor, and a combination of ionotronic luminescence and pressure sensing enables soft robots to sense and communicate[35].

Ionotronic liquid crystal device. An electro-optical device can modulate various properties of light, including the phase, polarization, amplitude and frequency[123]. Liquid crystals have enabled many electro-optical devices, most notably liquid crystal displays[124]. ITO is commonly used as the electrode, making liquid crystal devices fragile. Liquid crystal devices require the application of voltage and not the injection of electrons. A hydrogel ionotronic liquid crystal device is made of a layer of liquid crystal sandwiched between two elastomer layers and two hydrogel layers[36] (FIG. 3d). For example, the liquid crystal molecules in a cholesteric liquid crystal device form twisted domain structures that scatter light. Applying a voltage causes the liquid crystal molecules to align with the electric field and to transmit light (FIG. 3e). Therefore, the voltage can switch the device from an opaque state to a transparent state (FIG. 3f). Alternating voltage is applied to avoid the accumulation of space charges in the liquid crystals[125]. The hydrogel ionotronic liquid crystal device is soft and stretchable and remains functional under an equibiaxial stretch of 1.5 (FIG. 3f).

The high stretchability of hydrogel ionotronic liquid crystal devices enables a new mode of operation[36]; the device is switchable in response to a combination of electrical voltage and mechanical force. Applying a predesigned voltage keeps the liquid crystal layer in the opaque state, whereas stretching without increasing the voltage causes the liquid crystal layer to become transparent. Upon stretching, the area of the liquid crystal layer increases, and the thickness decreases, resulting in an increase in the electric field across the liquid crystal layer. The liquid crystal layer becomes transparent if the electric field is higher than the threshold above which liquid crystal molecules align.

The basic structure of hydrogel ionotronic liquid crystal devices can be fabricated using existing techniques, such as surface patterning, particle distribution, polymer dispersion of liquid crystals and polymer stabilization of liquid crystals. For example, a polymer-dispersed liquid crystal consists of a solid polymer matrix containing dispersed liquid crystal droplets[126] of the same refractive index. Sandwiching a polymer-dispersed liquid crystal layer within two hydrogel layers enables the fabrication of an all-solid but stretchable liquid crystal device.

Touchpad

Touchpads provide intuitive human–machine interfaces by combining sense and display. Mechanisms for sensing include resistive, capacitive, surface acoustic and infrared sensing[127–130]. Resistive and capacitive touch sensing have found broad applications in mobile phones, computers, ticketing machines and point-of-sale terminals[130]. Both touch sensing systems require transparent conducting films. A 1D hydrogel ionotronic touchpad consists of a strip of hydrogel with metallic electrodes at both ends, which are subjected to the same alternating voltage applied through current meters[37] (FIG. 4a). As a finger touches a point in the hydrogel, an ionic current flows between each of the ends and the point of touch. The capacitive coupling at each EDL causes the flow of an electronic current through a current meter. The two measured electronic currents determine the location of the point of touch. The capacitance of a finger is small (~100 pF)[131], and thus, even for a hydrogel with a thickness of 10 μm and a surface resistance of 100 Ω sq^{-1}, the *RC* delay is $\sim 10^{-3}$ s,

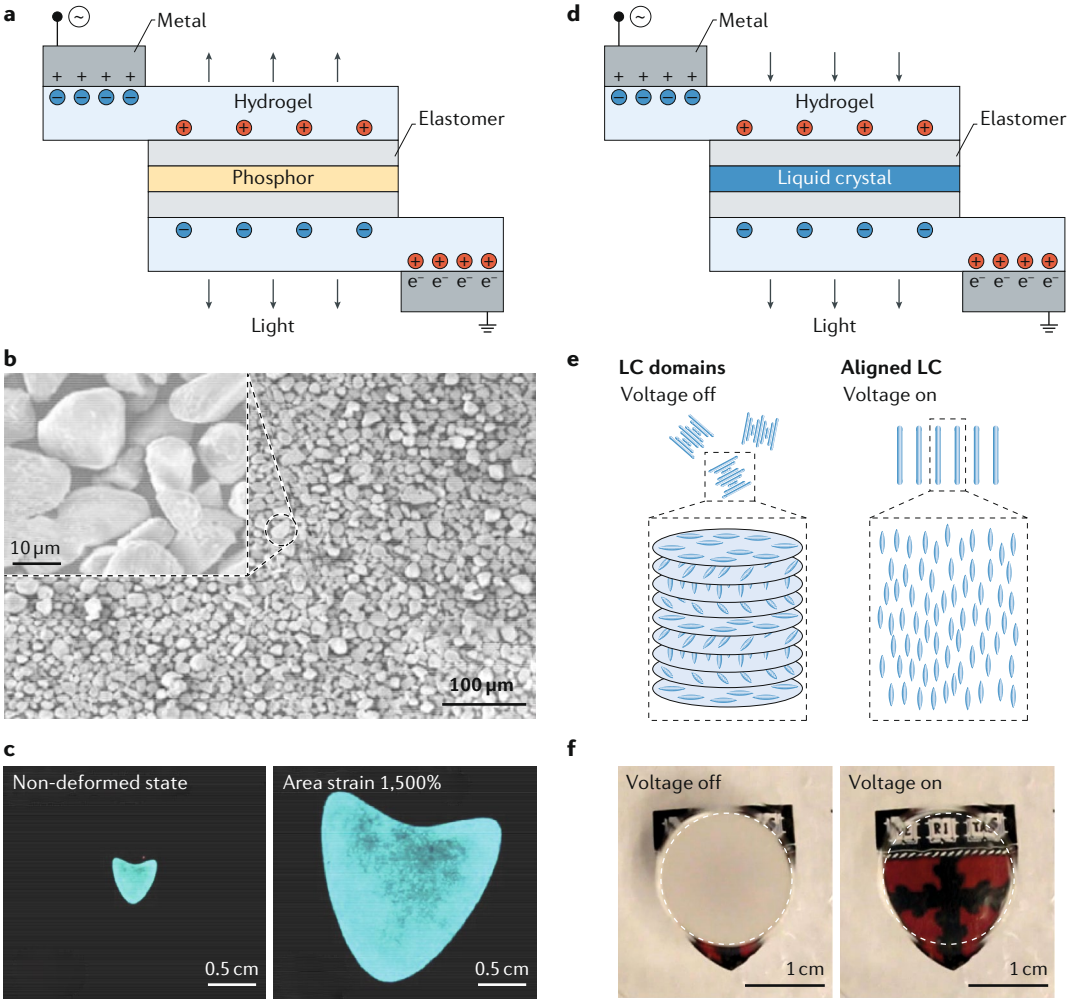

Fig. 3 | **Optoelectronic devices. a** | In an ionotronic luminescent device, a layer of phosphor is sandwiched between two transparent elastomers and then two transparent hydrogels. Applying an alternating voltage causes luminescence of the phosphor. **b** | Phosphor particles are hard but small and thus do not restrict the stretchability of the device. **c** | The intensity of light remains unchanged under an area strain of 1,500%. **d** | In an ionotronic liquid crystal (LC) device, a layer of LC is sandwiched between two elastomers and then two hydrogels. **e** | A cholesteric LC forms twisted domains and scatters light once the voltage is turned off; the domains unwind and transmit light once cyclic voltage is applied. **f** | A hydrogel ionotronic LC device is soft and stretchable, behaves like a light shutter and remains functional under an equibiaxial stretch of $\lambda = 1.5$. Panels **b** and **c** are adapted with permission from REF.[34], John Wiley and Sons. Panels **e** and **f** are adapted with permission from REF.[36], RSC.

which is smaller than the sampling instant (~10^{-2} s) of most measuring instruments. The hydrogel ionotronic touchpad is soft and stretchable, providing opportunities for the development of soft and seamless interfaces for human–machine interactions.

Triboelectric generator

A triboelectric nanogenerator (TENG) converts mechanical movement into electric current[132–134]. In a hydrogel ionotronic TENG, a hydrogel layer is encapsulated in an elastomeric cell and connected to an external load by a metal[38,39] (FIG. 4b). If a dielectric approaches and moves away from the elastomer cyclically, ions flow in the hydrogel, and the capacitive coupling of the EDL causes electrons to flow between the metal and the ground, generating an alternating current. Hydrogel ionotronic TENGs are highly stretchable and transparent and perform similar to TENGs based on electronic conductors[38–40].

Artificial eel

An electric eel can operate with a peak electric potential of up to 600 V and currents of 1 A (REF.[135]). This high power is generated by thousands of ionic gradients arranged in series[136]. Hydrogels can dissolve salts at a variety of concentrations and are ion-selective through the incorporation of polyelectrolyte networks. Hydrogels with different ion concentrations and hydrogels with reverse ion selectivity can be combined to form an ionic gradient to generate power. Thus, an artificial eel can be created by stacking a high-salinity hydrogel, a cation-selective hydrogel, a low-salinity hydrogel, an anion-selective hydrogel and a second high-salinity hydrogel in sequence[41] (FIG. 4c). Upon contact, an

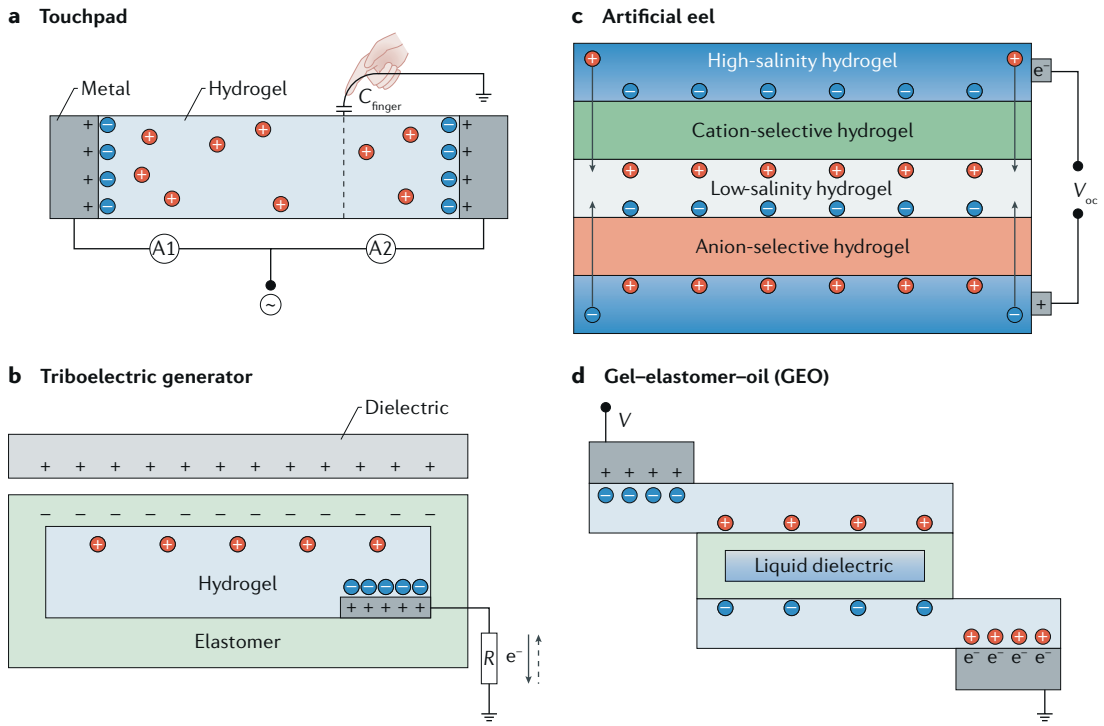

Fig. 4 | **Hydrogel ionotronic devices. a** | In a 1D touchpad, a hydrogel strip is connected at both ends to metallic electrodes, at which an AC voltage is applied through two current meters, A1 and A2. If a finger touches the hydrogel, an ionic current flows in the hydrogel between the point of touch and each electrode. Capacitive coupling at each electrical double layer (EDL) causes an electronic current to flow through each current meter. The current is inversely proportional to the distance between the electrode and the point of touch. **b** | In a triboelectric generator, a hydrogel is encapsulated in an elastomer cell and connected to an external load by an electrode. If a dielectric film contacts the elastomer, charges of opposite polarities coincide at the contacting surface. Removal of the dielectric film leaves excess charges behind at the elastomer–air interface. Subsequently, ions in the hydrogel accumulate at the hydrogel–elastomer surface, and charges of opposite polarities accumulate at the EDL between the hydrogel and the electrode, inducing electrons to flow between the electrode and the ground through the external load. If the dielectric film approaches the elastomer, electrons resume their flow but in the reverse direction. Repeated contact–separation movement leads to the generation of an alternating current through the load. **c** | In an artificial eel, stacking of a high-salinity hydrogel, a cation-selective hydrogel, a low-salinity hydrogel, an anion-selective hydrogel and a second high-salinity hydrogel leads to the formation of an ionic gradient, resulting in an open-circuit voltage, V_{oc}. **d** | In a gel–elastomer–oil (GEO) device, a layer of liquid dielectric is encapsulated in an elastomer cell and sandwiched between two hydrogels, which are connected to two metallic electrodes. If a voltage is applied between the two metallic electrodes, the electrostatic interaction bends the two layers of elastomer and displaces the liquid dielectric. C_{Finger}, capacitance of the finger; R, electrical resistance of the external load. Panel **a** is adapted with permission from REF.[37], AAAS. Panel **b** is adapted from REF.[38], CC-BY-4.0. Panel **c** is printed with permission from Caitlin C. Monney. Panel **d** is adapted with permission from REF.[42], AAAS.

ionically conductive pathway is established to form an ionic gradient, resulting in an open-circuit voltage, V_{oc}, which can be scaled up by stacking additional hydrogels in series, reaching up to 110 V (REF.[41]).

GEO devices

Liquids have long been used in machines to deliver power over a distance and have been integrated in dielectric elastomer actuators[137]. Electrohydrodynamic movements can further facilitate specific modes of operation in devices that integrate hydrogels, elastomers and liquid crystals[36]. The combination of a gel, an elastomer and oil allows for the creation of a soft device for a variety of applications (FIG. 4d). For example, GEO devices are being explored for the engineering of artificial muscles[42,43]. In such a device, the electrostatic attraction caused by an applied voltage displaces the liquid to the surrounding volume, generating a hydraulic pressure that deforms the actuator. The liquid dielectric can self-heal after electric breakdown[42].

Materials for hydrogel ionotronics

Hydrogels, salts, elastomers and metals are the main material components in hydrogel ionotronic devices (TABLE 1). Polyacrylamide (PAAm) hydrogels are easy to synthesize, highly stretchable and transparent. Although commonly used, polyacrylamide networks are covalently linked and thus do not heal after rupture. To provide healing, polyvinyl alcohol (PVA) and polyacrylic acid/alginate (PAAc/alginate) hydrogels can be used[31]. Salts include sodium chloride and lithium chloride, which have similar conductivities, but sodium chloride has better biocompatibility, while lithium chloride has better water retention. Elastomers are stretchable polymers and often transparent. Frequently used elastomers include VHB[138], polydimethylsiloxane (PDMS)

Table 1 | **Hydrogel ionotronic devices**

Device	Hydrogel network	Salt	Conductivity (S m^{-1})[a]	Elastomer	Metal	Working voltage[b]	Refs
Artificial muscle	PAAm	NaCl	10	3 M VHB	Copper	1–10 kV	21,22
	PAAm	LiCl	10	3 M VHB	Copper/Tin	1–10 kV	23-26
	PVA	LiCl	NA	3 M VHB	Aluminium	1–10 kV	27
	PAAm	LiCl	NA	Silicone	Copper	1–10 kV	28
Artificial skin	PAAm	NaCl	10	3 M VHB	NA	<1 V	29
	PAAm	NaCl	10	PDMS	Silver	NA	30
	PAAc/Alginate	NaCl	NA	3 M VHB	NA	NA	31
	PDMA	NaCl	NA	#	NA	1 V	32
	PAAc-co-DMAPS	NaCl	NA	3 M VHB	NA	NA	33
Artificial axon	PAAm	LiCl	10	3 M VHB	Copper	1 V	13
Electroluminescent device	PAAm	LiCl	10	3 M VHB	Aluminium	1–10 kV	34
	PAAm	LiCl	10	Ecoflex 00-30	Copper	1–10 kV	35
Liquid crystal device	PAAm	LiCl	10	3 M VHB	Aluminium	0.1–1 kV	36
Touchpad	PAAm	LiCl	1	3 M VHB	Platinum	1 V	37
Energy generator	PAAm	LiCl	10	3 M VHB/ PDMS	Aluminium/ Copper	1–100 V	38
	PVA	$Na_2B_4O_7$	1	3 M VHB	Platinum	1 V	39
	PVA	NA	NA	PDMS	Nickel	1–100 V	40
Artificial eel	PAAm/PAAm copolymer	NaCl	NA	##	Silver	0.1–100 V	41
GEO device	PAAm	LiCl	10	PDMS	NA	1–10 kV	42-44

DMAPS, 3-dimethyl(methacryloyloxyethyl) ammonium propane sulfonate; GEO, gel–elastomer–oil; LiCl, lithium chloride; NA, information unavailable; $Na_2B_4O_7$, sodium tetraborate; NaCl, sodium chloride; PAAc/alginate, polyacrylic acid/alginate; PAAm, polyacrylamide; PDMA, poly(*N*,*N*-dimethylacrylamide); PDMS, polydimethylsiloxane; PVA, polyvinyl alcohol; VHB, VHB by 3 M Inc. [a]Conductivity is represented as the order of magnitude. [b]Working voltage is represented as the order of magnitude. # indicates that polyethylene was used. ## indicates that an uncoated polyester was used.

and Ecoflex (Smooth-On). VHB is highly stretchable (~9 times its initial length) and transparent (>90% transparency at a thickness of 1 mm); however, the shape of VHB cannot be changed because it is already crosslinked. PDMS is less stretchable than VHB (~2 times its initial length) but is also transparent (>90% transparency at a thickness of 1 mm). Ecoflex is also highly stretchable (~7 times its initial length) but becomes opaque at thicknesses >1 mm. PDMS and Ecoflex can be synthesized from precursors and fabricated into various shapes with different thicknesses. The working voltage of hydrogel ionotronics ranges from ≤ 1 V to ~10 kV; to enable actuation, the voltage is typically ~1–10 kV; to provide power, the voltage ranges from 0.1–100 V; and for sensing, the voltage is <1 V. The voltage across the EDL should be restricted to approximately ± 1 V. Various electronic conductors have been used in hydrogel ionotronics; however, a systematic investigation of the electrochemistry at the interfaces between electronic conductors and hydrogels remains elusive. The working hypothesis is that the electrochemistry of these interfaces is similar to that of interfaces between electronic conductors and aqueous electrolytes.

Most hydrogels are fragile. A polyacrylamide hydrogel can be stretched several times its original length but ruptures at a much smaller stretch if the gel contains a crack that exceeds a few millimetres in length. This flaw sensitivity is common to all materials, but different materials are sensitive to flaws of different size[139]. The flaw sensitivity is related to the fracture energy (toughness) of a material. The fracture energy is ~1–10 J m^{-2} for tofu and jello and ~100 J m^{-2} for polyacrylamide hydrogels. By contrast, the fracture energy of natural rubber is >10,000 J m^{-2}. However, hydrogels can be made as tough as elastomers[116], allowing the possibility to create highly stretchable and tough hydrogels for hydrogel ionotronics[117,140–147]. The development of tough hydrogels requires specific material properties to achieve strong and stretchable adhesion between hydrophilic and hydrophobic polymer networks and to resist fatigue fracture under cyclic loading.

For a brittle solid, such as silica glass, all bonds between the atoms are strong. It is this unyielding strength that leads to brittleness. The fracture energy of such a solid can be described by the Griffith model[148] (FIG. 5a). Propagation of a crack in a brittle solid causes only one layer of atomic bonds to break; the remaining atomic bonds deform elastically and do not dissipate energy. Consequently, the fracture energy of a brittle solid corresponds to the covalent energy in a layer of atoms per unit area (~1 J m^{-2}). By contrast, an elastomer or a hydrogel is made of a network of crosslinked polymer

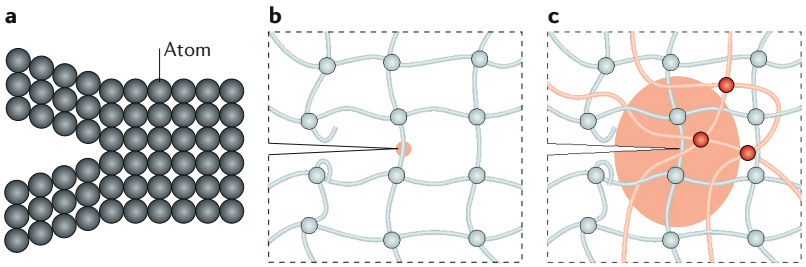

Fig. 5 | **Fracture energy. a** | The fracture energy of a brittle solid corresponds to the covalent energy of a layer of atoms per unit area. **b** | The fracture energy of a polymer network corresponds to the covalent energy of a layer of polymer chains per unit area. **c** | The facture energy of a polymer network can be increased if the polymer chains crossing the plane of a crack are strong enough to elicit hysteresis in the bulk of the network. Panel **c** is adapted from REF.[117], Macmillan Publishers Limited.

chains. Along each polymer chain, the monomer units strongly bind through chemical bonds similar to those in solids, but between polymer chains, the monomer units associate only weakly through physical interactions similar to those in liquids. Thus, at the molecular scale, an elastomer or a hydrogel is a solid–liquid hybrid. The fracture energy of a stretchable polymer network can be described by the Lake–Thomas model[149] (FIG. 5b). The interaction between the polymer chains is weak, and when stretching the network, just before the polymer chain breaks at the front of the crack, each monomer unit along the polymer chain has a strength near that of a chemical bond. Breaking of the chain at a single bond then triggers the stored energy in the entire chain to be dissipated. Thus, the fracture energy of a polymer network corresponds to the covalent energy of a layer of polymer chains per unit area (~10–100 J m^{-2}) and depends on the length of the chains in the network.

The fracture energy of a polymer network can be increased if the polymer chains across the plane of the crack are strong enough to elicit hysteresis in the bulk of the network[150] (FIG. 5c), which stems from sacrificial bonds. The hysteresis dissipates energy and contributes to the fracture energy. A high fracture energy is achieved by sacrificial bonds that break when the hydrogel is stretched to an intermediate level[117]. If the sacrificial bonds break under low stretching, a negligible amount of energy is dissipated through hysteresis, and thus, the fracture energy is low. If the sacrificial bonds break under high stretching, the polymer network ruptures without breaking the sacrificial bonds in a large volume of the material, and thus, the fracture energy is low as well. The synergy between crack bridging and bulk hysteresis is inherent to tough materials, such as ductile metals, tough ceramics, ceramic matrix composites and rubber-filled plastics[151–154]. A variety of physical sacrificial bonds have been explored for the fabrication of tough hydrogels and elastomers[117,140–147,155].

Adhesion, water retention and fatigue

The major challenges to overcome for materials to be applied in hydrogel ionotronics are achieving strong adhesion between hydrogels and hydrophobic elastomers, water retention and fatigue resistance under cyclic loads.

Adhesion. An integrated circuit functions by integrating dissimilar components. Hydrogel ionotronics integrate hydrogels with other materials, most notably metals and elastomers. Hydrogels function as conductors, and elastomers function as dielectrics and seals, retarding dehydration of the hydrogels if the device is in contact with air or the exchange of solutes if the device is immersed in aqueous solution. Therefore, an elastomer must have low solubility and diffusivity of water and solutes. Moreover, many hydrogel ionotronic devices require that both hydrogels and elastomers are stretchable and transparent. To design an ionotronic device based on hydrogels and elastomers, strong adhesion between hydrophilic and hydrophobic polymer networks needs to be achieved without sacrificing stretchability and transparency.

Hydrogels and elastomers often have an adhesion energy (typically <1 J m^{-2}) lower than the fracture energy of tough elastomers and hydrogels (typically >1,000 J m^{-2})[156]. However, it is possible to design hydrogels and elastomers with an adhesion energy as high as the bulk fracture energy[51–53,157,158]. Dissimilar materials adhere through physical interactions, chemical bonds or combinations thereof[159]. An adhesive (for example, epoxy or cyanoacrylate) and an adherend (for example, an elastomer, plastic, metal or ceramic) can achieve appreciable adhesion energy without chemical bonds if the physical interactions are sufficiently strong and dense. Every atom or monomer unit at the interface between the adhesive and adherend carries a specific load to establish adhesion (FIG. 6a). However, this non-covalent adhesion is particularly weak between hydrogels and elastomers. The water molecules in the hydrogel are densely packed, but they do not carry load because they behave similar to how they behave in liquid water (FIG. 6b). Moreover, the weak bonds between the loosely packed polymer chains in the hydrogel and elastomer do not activate the Lake–Thomas mechanism or elicit sufficient hysteresis in the bulk of the material.

The Lake–Thomas mechanism for adhesion can be activated between a hydrogel and an elastomer through the formation of strong inter-network bonds (FIG. 6c), which need to be as sparse as the crosslinks within the individual networks to maintain stretchability and transparency. Inter-network bonds denser than the crosslinks inside the hydrogel can increase the adhesion but decrease the stretchability along the plane of the interface. Moreover, an adhesion energy higher than the fracture energy of the hydrogel is in general useless because rupture can simply occur inside the hydrogel near the interface. The adhesion energy can be further increased by the presence of sacrificial bonds in the bulk of the hydrogel and the elastomer (FIG. 6d), and if the inter-network bonds are strong enough to elicit hysteresis in the bulk of the material[157] (FIG. 6e). These conditions allow for the adhesion energy between a hydrogel and an elastomer to be comparable to the fracture energy of the hydrogel.

The third network that is formed at the interface between the hydrogel and the elastomer establishes three types of topology: topological entanglement

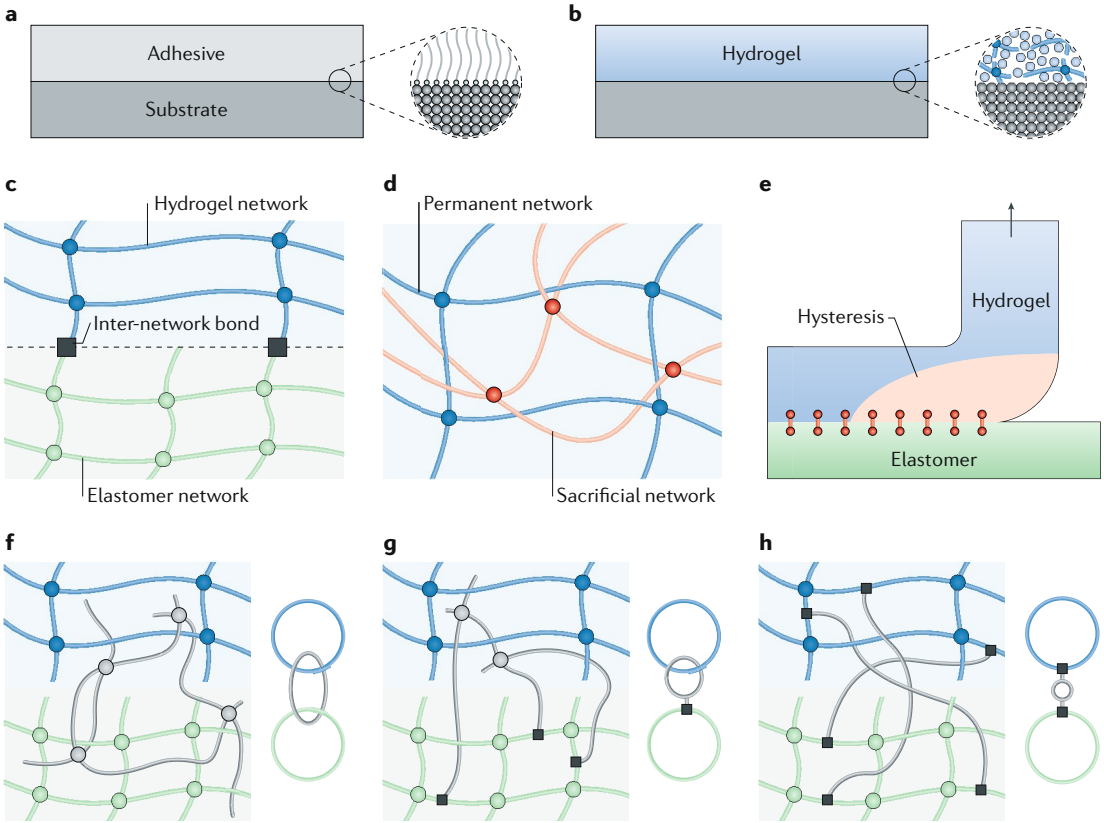

Fig. 6 | **Hydrophilic–hydrophobic adhesion.** Adhesion between a plastic adhesive and a dense substrate is established through a high density of non-covalent bonds, with the individual bonds being of modest strength (panel **a**). In a hydrogel, polymer chains are sparse (panel **b**). Water molecules have the same properties as in liquid water and are densely packed. The adhesion energy is almost the same as the fracture energy if the two networks form strong, sparse inter-network bonds (panel **c**). A sacrificial network enables hysteresis in the bulk of a hydrogel (panel **d**). The adhesion energy is increased if the inter-network bonds are strong enough to elicit hysteresis in the bulk of a hydrogel (panel **e**). Adhesion can be further increased if a third network is in topological entanglement with the two pre-existing networks (panel **f**), in topological entanglement with one pre-existing network and strongly and sparsely bonded to the second pre-existing network (panel **g**) or strongly and sparsely bonded to both pre-existing networks (panel **h**). Panel **e** is adapted from REF.[157], Macmillan Publishers Limited. Panel **f** is adapted with permission from REF.[160], John Wiley and Sons.

with the two pre-existing networks[160] (FIG. 6f), topological entanglement with one pre-existing network and strong bonds with the second pre-existing network (FIG. 6g), or strong bonds with both pre-existing networks (FIG. 6h). The adhesion energy is comparable to the fracture energy if the third network and the inter-network bonds are strong enough to activate the Lake–Thomas mechanism and elicit hysteresis in the bulk of the network. If the third network forms a topological entanglement with the two pre-existing networks (FIG. 6h), stretchable and strong adhesion is achieved without the need for functional groups from the two pre-existing networks. This method of adhesion is called topological adhesion (or topohesion). In this case, the third network functions as a molecular suture. The interplay of cohesion, adhesion and topohesion offers opportunities for the design of integrated polymer devices.

The adhesion between a hydrogel and an elastomer can be improved by treating the elastomer surface with oxygen plasma or ozone[161–163] (FIG. 7a). The van der Waals interactions between water molecules and the $-CH_3$ groups of the hydrophobic polymer chains are the main interactions in an elastomer (FIG. 7b). Hydrophilic treatment converts the $-CH_3$ groups into –OH groups, leading to the formation of a nanometre-thick hydrophilic layer[164] and promoting the spread of the hydrogel precursor (FIG. 7c). The hydrophilic surface easily degrades in air but is preserved when in contact with water[165]. However, such a treatment usually does not lead to high adhesion energy. Even if a monolayer of water molecules are strongly bonded to the surface of the elastomer, the water molecules in the bulk are still as weakly bonded as in liquid water. The treatment does promote stronger physical association between the polymer chains in the hydrogels and the elastomer, but still not strong enough to elicit the Lake–Thomas mechanism or significant hysteresis in the bulk. Separation of the water–elastomer interface results in two new interfaces (the water–air and elastomer–air interfaces). For example, the water–PDMS, water–air and PDMS–air interfacial energies are ~0.04 J m^{-2}, ~0.07 J m^{-2} and ~0.02 J m^{-2}, respectively[166], with an adhesion energy between the elastomer and hydrogel of ~0.05 J m^{-2}.

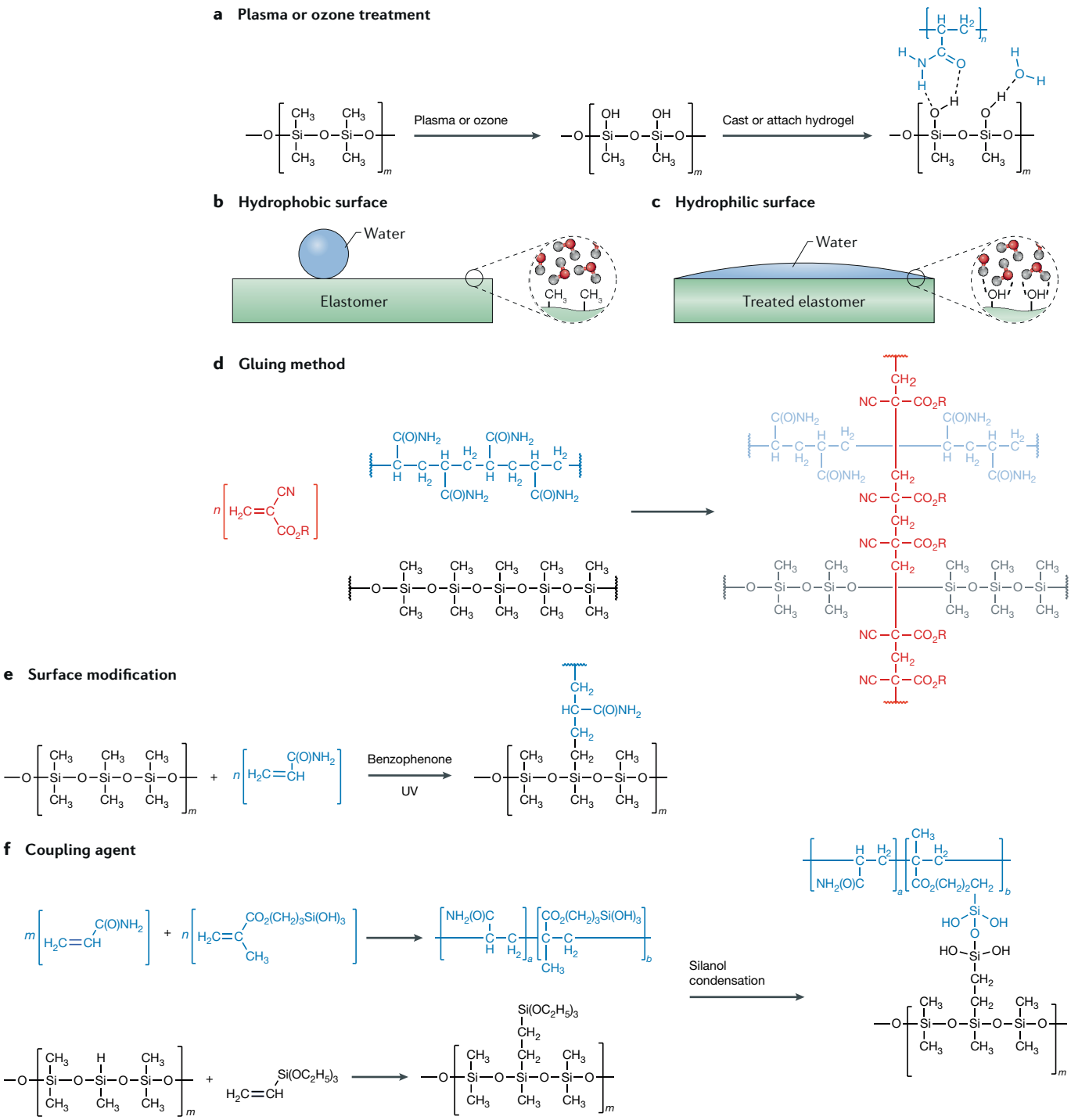

Fig. 7 | **Chemistry of hydrogel–elastomer adhesion. a** | Plasma or ozone treatment converts $-CH_3$ groups on the elastomer chains into –OH groups. Following the casting and curing of hydrogel precursors, the hydrogel adheres to the elastomer through physical interactions. **b** | The $-CH_3$ group on an elastomer is hydrophobic, repelling water, leading to the formation of droplets. **c** | Treatment of an elastomer to convert the hydrophobic $-CH_3$ groups into hydrophilic –OH groups leads to water spreading and the formation of interfacial bonds that do not affect the intermolecular bonds inside of water. **d** | Diluted cyanoacrylate can be applied between a preformed hydrogel and a preformed elastomer. The monomers polymerize and form a third network. **e** | The surface of an elastomer can be treated with benzophenone. Hydrogel precursors are cast on the surface and exposed to UV irradiation. One part of benzophenone reacts with all the oxygen at the hydrogel–elastomer interface, and the other part initiates free radicals on the elastomer network that participate in the polymerization of the hydrogel network. **f** | Silane coupling agents can be added to the hydrogel and elastomer precursors. During network formation, the coupling agents are incorporated into the polymer chains, but they do not condensate. Following a manufacturing process, the coupling agents condensate, add crosslinks to the networks and generate adhesion between the networks.

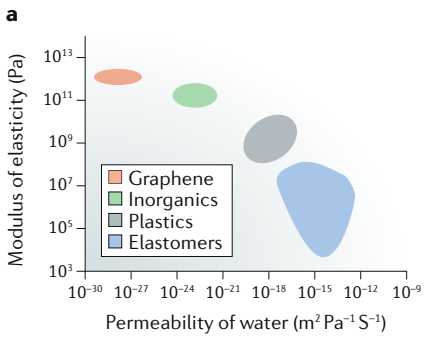

b

Salt	RH (%) at 25 °C
LiCl	11.3
NaCl	75.1
KCl	84.2
$MgCl_2$	32.7
K_2SO_4	97.0

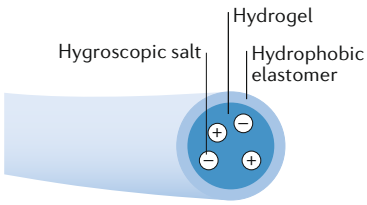

Fig. 8 | **Water retention. a** | Modulus of elasticity and water permeability of different materials. **b** | The relative humidity (RH) of saturated aqueous salt solutions. **c** | A combination of a hydrogel, a hygroscopic salt and a hydrophobic elastomer. Panels **a** and **c** are adapted with permission from REF.[55], American Chemical Society.

With plasma or ozone treatment of PDMS (assuming that the surface tension is increased to that of water), the adhesion is ~0.14 J m^{-2} when only interfacial bonding and not effects of chain breaking and bulk hysteresis are considered.

A gluing method can be applied, in which cyanoacrylate monomers form polymer chains at the interface between the hydrogel and the elastomer[52] (FIG. 7d). The cyanoacrylate adhesive is diluted to avoid rapid polymerization, which would result in a bulky and brittle layer[167]. The polymerized cyanoacrylate network is strong enough to elicit large hysteresis in the hydrogel bulk[168]. Depending on the hydrogel, the adhesion energy can reach up to 2,000 J m^{-2}. The gluing method is characterized by fast bonding and high toughness, and extended curing or crosslinking is not required. The instant nature of this reaction is important for time-critical applications such as rapid prototyping. However, a non-acidic environment and preformed materials are required. Moreover, the mechanism of adhesion by gluing has not yet been identified.

Adhesion can also be improved by using benzophenone to modify the surface of the elastomer[51] (FIG. 7e). Benzophenone reacts with dissolved oxygen to alleviate the inhibition effect[169] and acts as a photoinitiator to covalently anchor the hydrogel network onto the elastomer network[170,171]. This method is broadly applicable to various types of elastomers and hydrogels and results in high interfacial toughness (>1,000 J m^{-2}). Such surface modification demands that the hydrogels are cast on preformed elastomers, which requires an oxygen-free environment for polymerization of the hydrogel. Moreover, the elastomer cannot be coated on a preformed hydrogel of arbitrary shape.

Alternatively, silanes can be incorporated as coupling agents into the precursors of both the hydrogel and elastomer[53] (FIG. 7f). During formation of the networks, the coupling agents are covalently incorporated into the networks but do not condensate. Following a manufacturing process, the coupling agents condensate, add crosslinks to the individual networks and form covalent bonds between the networks. The coupling agent method achieves strong adhesion independent of the sequence of network formation and is compatible with a variety of manufacturing processes. The bonding kinetics can be tuned by changing the temperature or pH or by adding surfactants. However, a post-condensation time is required, which is time consuming and difficult to implement in the manufacturing process.

Finally, nanoparticles can be added to the hydrogel–elastomer interface to increase adhesion to ~10 J m^{-2} (REF.[172]).

Water retention. Electronics are prone to moisture. Conventional rigid electronics are hermetically sealed with inorganic coatings, but for stretchable electronics, alternative strategies must be applied. However, stretchable materials with low water permeability do not yet exist[55] (FIG. 8a). At the molecular level, stretchability and permeability are inextricably linked. Only materials that contain long and flexible polymer chains are capable of large and elastic stretching. To be stretchable, individual polymer chains need to undergo continuous thermal motion. Consequently, small molecules, such as water and oxygen, can diffuse in an elastomer as readily as in a polymer liquid.

Hydrogels are susceptible to dehydration in air. Dissociation of a hygroscopic salt in water results in the formation of hydrated ions, decreasing the vapour pressure[17,173] (FIG. 8b). The salts further stabilize the water in the hydrogels. For example, a polyacrylamide hydrogel containing 12 M lithium chloride retains water at a humidity of 10%[54]. Hydrogels containing hygroscopic salts do not dry out in air but swell and de-swell in response to fluctuations in the ambient humidity. The corresponding fluctuation in water content causes changes in the electrical properties. Alternatively, an ionogel, that is, a polymer network swollen with an ionic liquid[174], can be used because it is non-volatile in a vacuum[175] and can perform over a wide range of temperatures, depending on the type of ionic liquid[176].

Hydrogels can also be coated with a thin film of elastomer to retain water[29,51,55]. At the scale of the monomer units, the elastomer is liquid-like and thus allows the diffusion of molecules that are smaller than the mesh size of the elastomer. Thus, coating with an elastomer slows but does not stop dehydration. However, the combination of a hygroscopic salt and hydrophobic coating can eliminate dehydration[55] (FIG. 8c). Under low-humidity conditions, water molecules diffuse out of the hydrogel through the elastomer coating. An elastomer

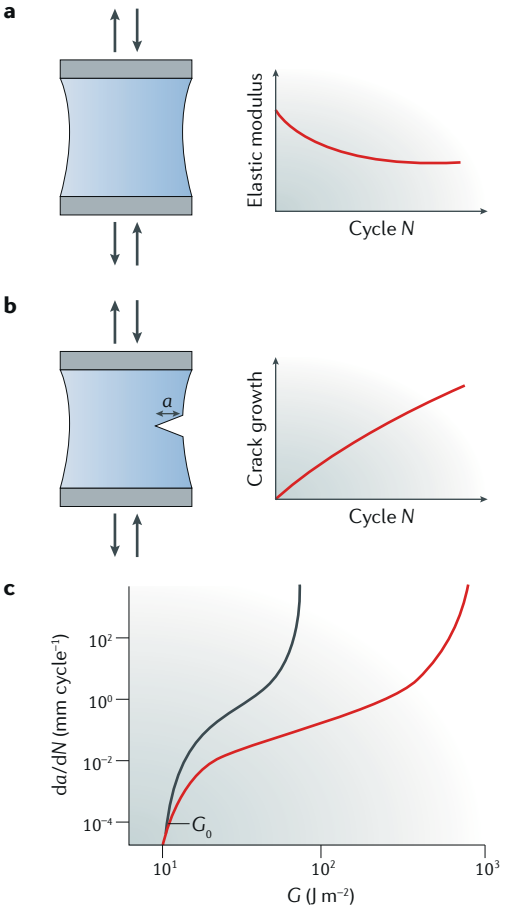

Fig. 9 | **Fatigue of hydrogels. a** | Exposing an uncut hydrogel sample to a cyclic load leads to irreversible changes in certain mechanical properties, such as the elastic modulus. These changes are called fatigue damage. **b** | Exposing a pre-cut hydrogel sample to a cyclic load leads to the gradual extension of the crack, *a*, which is called fatigue fracture. **c** | The extension of the crack per cycle, d*a*/d*N*, as a function of energy release rate, *G*. The black curve corresponds to a hydrogel that contains a single permanent network, and the red curve corresponds to a hydrogel that contains a hybrid of a permanent network and a sacrificial network. Adapted with permission from REF.[67], American Chemical Society.

can be designed with a specific thickness to increase the diffusion time of the water molecules so that the ambient humidity already becomes high or low before the hydrogel loses or absorbs water. Thereby, the hydrogel maintains a constant water content.

A hydrogel also exchanges solutes with the environment, for example, if it is immerged in an aqueous solution or in contact with a wet surface, such as a tissue. Sealing the hydrogel with a thin film of elastomer can also prevent mass exchange. For example, the diffusion of ions out of a salt-containing hydrogel, which increases the resistance of the hydrogel in a deionized water bath, can be prevented by coating with butyl rubber[55]. A thin adherent elastomer coating further enables a hydrogel to sustain temperatures >100 °C without boiling[53], similar to pressure cooking. These approaches allow for the design of wearable, washable and ironable hydrogel ionotronic devices.

Fatigue. A metal wire can be bent back and forth repeatedly, but after a certain number of cycles, it breaks. Fracture under cyclic load, called fatigue, has been well studied for load-carrying materials, such as metals, plastics, ceramics and composites[177,178]. Less is known about fatigue in hydrogels. However, the investigation of fatigue and the development of fatigue-resistant hydrogels are important for applications of load-carrying hydrogels in medicine and engineering.

The fatigue of hydrogels can be studied using either uncut or pre-cut samples[67]. Exposing an uncut hydrogel sample to a cyclic load leads to irreversible changes in the mechanical properties of the hydrogel, for example, of the elastic modulus; these changes are called fatigue damage (FIG. 9a). A hydrogel that is free of fatigue damage usually contains a permanent network and a few transient, reversible bonds[59,60,62,66]. The permanent network enables entropic elasticity, and the reversible bonds allow for hysteresis and increase the toughness. A pure polyacrylamide hydrogel is close to perfectly elastic but still exhibits slight hysteresis under loading–unloading cycles[57]. In a hydrogel that contains both a polyacrylamide network and PVA chains, the PVA chains interact with each other through hydrogen bonds, leading to pronounced hysteresis[179]. Such a hydrogel recovers its initial stress–strain curve after 5,000 loading cycles[67]. Depending on the chemical composition, the recovery time can vary and can be accelerated by increasing the temperature. For example, an alginate/polyacrylamide hydrogel exhibits pronounced hysteresis in the first cycle of loading and unloading but less hysteresis in subsequent cycles, with recovery occurring only at increased temperatures[117].

Exposing a pre-cut hydrogel sample to a cyclic load causes a gradual extension of the crack, which is called fatigue fracture (FIG. 9b). Fatigue fracture has been studied for four types of hydrogels: pure polyacrylamide hydrogels[56], alginate/polyacrylamide hydrogels[57], poly(2-acrylamido-2-methylpropane sulfonic acid)/polyacrylamide (that is, double-network) hydrogels[58] and polyacrylamide/PVA hydrogels[67]. The crack always propagates cycle-by-cycle, and thus, 'fatigue-free' hydrogels do not exist by this definition. Therefore, both fatigue damage and fatigue fracture should be considered in the hydrogel design.

The chemical composition of a hydrogel has a profound effect on fatigue fracture. The crack extension per cycle, d*a*/d*N*, is an increasing function of the energy release rate, *G* (FIG. 9c). If d*a*/d*N* is large, *G* approaches the fracture energy, whereas if d*a*/d*N* is small, *G* approaches the fatigue threshold, G_0, below which the crack does not extend upon cyclic loading. In hydrogels that contain both a permanent network and sacrificial network, the sacrificial network can greatly increase the fracture energy but negligibly affects the fatigue threshold[58,67]. At a load above the fatigue threshold, the crack extension per cycle in a tough hydrogel is smaller than in a brittle hydrogel by orders of magnitude (FIG. 9c).

Fatigue fracture has been studied only for hydrogels that contain covalent networks, which enable entropic elasticity and thus recovery. In hydrogels that consist of only physical networks, the networks can self-heal after damage. However, most existing self-healing hydrogels are weak and deform under small loads, behaving like a plastic liquid[61]. Hydrogels can be designed so that the physical networks are strong enough to provide the elasticity that facilitates recovery. For example, strong and weak ionic bonds can be combined in a hydrogel; strong bonds provide crosslinks, enabling elasticity, and weak bonds can be reversibly formed and broken to induce energy dissipation and toughen the hydrogel[180]. However, the fatigue behaviour of such hydrogels remains elusive.

Conclusions and outlook

Artificial intelligence, synthetic biology, augmented reality, machine learning, persistent deep-brain recording and stimulation, cyborgs and digiceuticals represent technologies at the interface between natural and artificial, and the integration of humans and computers already plays a central role in the development of wearable and implantable devices. Synthetic hydrogels mimic living tissues in terms of mechanical, chemical, optical and electrical properties and therefore constitute key players for the integration of humans and machines. First-generation hydrogel ionotronic devices feature hydrogels as stretchable, transparent, ionic conductors. The unique combination of transparency, stretchability and ionic conductivity enables high-voltage ionotronics, high-speed artificial axons, ionotronic luminescence, highly stretchable liquid crystal devices and touchpads. Furthermore, the development of hydrogel ionotronic devices has posed fundamental challenges to the chemistries and mechanics of hydrogels, for example, strong and stretchable adhesion, water retention and fatigue resistance. Hydrogels can further be used as soft electrolytes in electrophysiological measurements to connect tissues and metals[19,20], as soft substrates for electrical components[181] and as soft electronic conductors composed of conductive polymers[182–184].

Next-generation hydrogel ionotronics are envisioned to be implemented in applications such as soft robots and wearable and implantable devices. Many immediate opportunities exist, for example, in inventing new concepts of hydrogel ionotronic devices, in advancing the science of hydrogels and in developing integration and manufacturing. Soft robots require soft sensors and soft interconnects. However, many existing soft robots contain hard components, limiting their performance and application. For example, the movements of fingers or knees of an exoskeleton are restricted by the dangling wires that connect the respective components to the microprocessors[185,186]. Hydrogel-based devices could provide soft connecting components for soft and stretchable robots. The mechanical properties of electronic conductors used to establish human–machine interfaces often do not match those of soft tissues, such as the brain, heart or skin. Hydrogels can be applied to provide seamless human–machine interfaces.

Many hydrogel ionotronic devices integrate hydrogels and elastomers and employ planar laminated structures; however, such devices suffer from poor adhesion between hydrogels and elastomers. New adhesion methods and manufacturing processes will improve the integration of hydrogels and elastomers and allow for the design of devices with complex shapes. For example, ionotronic luminescent devices could be integrated into wearable and washable textiles. Currently available hydrogel devices that respond to stimuli such as temperature, electric and magnetic fields or light work only in aqueous environments; however, coating hydrogels with elastomers could enable the operation of such devices in air. Hydrogel ionotronic devices also rely on non-Faradaic coupling between mobile electrons and mobile ions. Devices that require voltage but not electron injection can be readily implemented using hydrogels. Specific designs, such as the rocking-chair design, enable hydrogels to transmit power to light-emitting diodes[13]. Many existing devices are based on the hypothesis that the electrochemistry of a metal–hydrogel interface is similar to that of a metal–water interface. This hypothesis should be studied to better understand the effect of polymers on the interface.

A hydrogel–elastomer laminate in an artificial muscle operates under high voltage. Ions and water molecules can migrate from the hydrogel to the elastomer, causing electric breakdown. Thus, ideal combinations of materials need to be explored to engineer devices with long lifetimes. Electrical breakdown and water treeing in polymers have been extensively studied for applications in high-voltage cables[164], providing useful input for studying polymer behaviour in hydrogel ionotronics. Current hydrogel ionotronic devices mainly rely on manual assembly. The lack of robust techniques for rapid prototyping has become a bottleneck to innovation. Batch synthesis can be applied to produce devices with feature sizes of ~1 mm; however, printing would enable the fast and low-cost mass production of devices at the sub-millimetre scale. For example, 3D extrusion printing is a versatile method compatible with a variety of materials, including hydrogels[165,187]. Miniaturization by printing could facilitate the production of hydrogel ionotronic strain sensors[97], soft somatosensitive actuators[188] and capacitive, soft strain-sensing[189], tactile-sensing and motion-sensing suits[102].

Ionotronic devices can also function when the hydrogels are exposed to solvents other than water, for example, ionic liquids or ethylene glycol[21,28]. Ionogels are non-volatile at a wide range of temperatures and thus can extend the range of possible applications[174,175,190–192]. For example, ionogels made of various polymer networks and ionic liquids[176,193,194] can be integrated with dielectric elastomers and other materials. The development of these materials, along with methods of integration, is wide open for exploration. Advances in hydrogel ionotronics will help to create deep integration between the natural and the artificial.

Published online: 14 May 2018

1. Lacour, S. P., Courtine, G. & Guck, J. Materials and technologies for soft implantable neuroprostheses. *Nat. Rev. Mater.* **1**, 16063 (2016).
2. Someya, T., Bao, Z. & Malliaras, G. G. The rise of plastic bioelectronics. *Nature* **540**, 379 (2016).
3. Zhang, A. & Lieber, C. M. Nano-bioelectronics. *Chem. Rev.* **116**, 215–257 (2015).
4. Chen, R., Canales, A. & Anikeeva, P. Neural recording and modulation technologies. *Nat. Rev. Mater.* **2**, 16093 (2017).
5. Feiner, R. & Dvir, T. Tissue–electronics interfaces: from implantable devices to engineered tissues. *Nat. Rev. Mater.* **3**, 17076 (2017).
6. Jeong, J.-W. et al. Soft materials in neuroengineering for hard problems in neuroscience. *Neuron* **86**, 175–186 (2015).
7. Manthiram, A., Yu, X. & Wang, S. Lithium battery chemistries enabled by solid-state electrolytes. *Nat. Rev. Mater.* **2**, 16103 (2017).
8. Mohtadi, R. & Orimo, S.-i. The renaissance of hydrides as energy materials. *Nat. Rev. Mater.* **2**, 16091 (2017).
9. El-Kady, M. F., Shao, Y. & Kaner, R. B. Graphene for batteries, supercapacitors and beyond. *Nat. Rev. Mater.* **1**, 16033 (2016).
10. Sheberla, D. et al. Conductive MOF electrodes for stable supercapacitors with high areal capacitance. *Nat. Mater.* **16**, 220 (2017).
11. Irvine, J. T. et al. Evolution of the electrochemical interface in high-temperature fuel cells and electrolysers. *Nat. Energy* **1**, 15014 (2016).
12. Park, M., Ryu, J., Wang, W. & Cho, J. Material design and engineering of next-generation flow-battery technologies. *Nat. Rev. Mater.* **2**, 16080 (2017).
13. Yang, C. H. et al. Ionic cable. *Extreme Mechan. Lett.* **3**, 59–65 (2015).
14. Chun, H. & Chung, T. D. Iontronics. *Ann. Rev. Anal. Chem.* **8**, 441–462 (2015).
15. Leger, J., Berggren, M. & Carter, S. *Iontronics: Ionic Carriers in Organic Electronic Materials and Devices*. (CRC Press, 2016).
16. Bisri, S. Z., Shimizu, S., Nakano, M. & Iwasa, Y. Endeavor of iontronics: from fundamentals to applications of ion-controlled electronics. *Adv. Mater.* (2017).
17. Stokes, R. H. & Robinson, R. A. Ionic hydration and activity in electrolyte solutions. *J. Am. Chem. Soc.* **70**, 1870–1878 (1948).
18. Bard, A. J., Inzelt, G. & Scholz, F. *Electrochemical Dictionary*. (Springer Science & Business Media, 2008).
19. Devlin, P. H. et al. Electrode array system for measuring electrophysiological signals. US Patent US6394953B1 (2002).
20. Goding, J. A., Gilmour, A. D., Aregueta-Robles, U. A., Hasan, E. A. & Green, R. A. Living bioelectronics: strategies for developing an effective long-term implant with functional neural connections. *Adv. Funct. Mater.* **28**, 1702969 (2018).
21. Keplinger, C. et al. Stretchable, transparent, ionic conductors. *Science* **341**, 984–987 (2013).
22. Suo, Z. Journal Club Theme of September 2013: Stretchable Ionics. *iMechanica* http://imechanica.org/node/15218 (2013).
23. Bai, Y. et al. Cyclic performance of viscoelastic dielectric elastomers with solid hydrogel electrodes. *Appl. Phys. Lett.* **104**, 062902 (2014).
24. Chen, B. et al. Stretchable and transparent hydrogels as soft conductors for dielectric elastomer actuators. *J. Polym. Sci. B Polym. Phys.* **52**, 1055–1060 (2014).
25. Li, T. et al. Fast-moving soft electronic fish. *Sci. Adv.* **3**, e1602045 (2017).
26. Zhang, C. et al. Electromechanical deformation of conical dielectric elastomer actuator with hydrogel electrodes. *J. Appl. Phys.* **119**, 094108 (2016).
27. Xu, C., Li, B., Xu, C. & Zheng, J. A novel dielectric elastomer actuator based on compliant polyvinyl alcohol hydrogel electrodes. *J. Mater. Sci. Mater. Electron.* **26**, 9213–9218 (2015).
28. Haghiashtiani, G., Habtour, E., Park, S.-H., Gardea, F. & McAlpine, M. C. 3D printed unimorph dielectric elastomer actuators. *Extreme Mechan. Lett.* **21**, 1–8 (2018).
29. Sun, J. Y., Keplinger, C., Whitesides, G. M. & Suo, Z. Ionic skin. *Adv. Mater.* **26**, 7608–7614 (2014).
30. Sarwar, M. S. et al. Bend, stretch, and touch: locating a finger on an actively deformed transparent sensor array. *Sci. Adv.* **3**, e1602200 (2017).
31. Lei, Z., Wang, Q., Sun, S., Zhu, W. & Wu, P. A bioinspired mineral hydrogel as a self-healable, mechanically adaptable ionic skin for highly sensitive pressure sensing. *Adv. Mater.* **29**, 1700321 (2017).
32. Lei, Z., Wang, Q. & Wu, P. A multifunctional skin-like sensor based on a 3D printed thermo-responsive hydrogel. *Mater. Horiz.* **4**, 694–700 (2017).
33. Lei, Z. & Wu, P. A supramolecular biomimetic skin combining a wide spectrum of mechanical properties and multiple sensory capabilities. *Nat. Commun.* **9**, 1134 (2018).
34. Yang, C. H., Chen, B., Zhou, J., Chen, Y. M. & Suo, Z. Electroluminescence of giant stretchability. *Adv. Mater.* **28**, 4480–4484 (2016).
35. Larson, C. et al. Highly stretchable electroluminescent skin for optical signaling and tactile sensing. *Science* **351**, 1071–1074 (2016).
36. Yang, C. H., Zhou, S., Shian, S., Clarke, D. R. & Suo, Z. Organic liquid-crystal devices based on ionic conductors. *Mater. Horiz.* **4**, 1102–1109 (2017).
37. Kim, C.-C., Lee, H.-H., Oh, K. H. & Sun, J.-Y. Highly stretchable, transparent ionic touch panel. *Science* **353**, 682–687 (2016).
38. Pu, X. et al. Ultrastretchable, transparent triboelectric nanogenerator as electronic skin for biomechanical energy harvesting and tactile sensing. *Sci. Adv.* **3**, e1700015 (2017).
39. Parida, K. et al. Highly transparent, stretchable, and self-healing ionic-skin triboelectric nanogenerators for energy harvesting and touch applications. *Adv. Mater.* **29**, 1702181 (2017).
40. Xu, W. et al. Environmentally friendly hydrogel-based triboelectric nanogenerators for versatile energy harvesting and self-powered sensors. *Adv. Energy Mater.* **7**, 1601529 (2017).
41. Schroeder, T. B. et al. An electric-eel-inspired soft power source from stacked hydrogels. *Nature* **552**, 214 (2017).
42. Acome, E. et al. Hydraulically amplified self-healing electrostatic actuators with muscle-like performance. *Science* **359**, 61–65 (2018).
43. Kellaris, N., Venkata, V. G., Smith, G. M., Mitchell, S. K. & Keplinger, C. Peano-HASEL actuators: muscle-mimetic, electrohydraulic transducers that linearly contract on activation. *Sci. Robot.* **3**, eaar3276 (2018).
44. Keplinger, C. Journal Club for February 2018: HASEL artificial muscles for high-speed, electrically powered, self-healing soft robots. *iMechanica* http://imechanica.org/node/22096 (2018).
45. Wichterle, O. & Lim, D. Hydrophilic gels for biological use. *Nature* **185**, 117 (1960).
46. Wichterle, O., Lim, D. & Dreifus, M. On the problem of contact lenses. *Ceskoslovenska Oftalmol.* **17**, 70 (1961).
47. Dubrovskii, S., Afanas' eva, M., Lagutina, M. & Kazanskii, K. Comprehensive characterization of superabsorbent polymer hydrogels. *Polym. Bull.* **24**, 107–113 (1990).
48. Thiele, J., Ma, Y., Bruekers, S., Ma, S. & Huck, W. T. 25th Anniversary article: designer hydrogels for cell cultures: a materials selection guide. *Adv. Mater.* **26**, 125–148 (2014).
49. Lee, K. Y. & Mooney, D. J. Hydrogels for tissue engineering. *Chem. Rev.* **101**, 1869–1880 (2001).
50. Hoffman, A. S. Hydrogels for biomedical applications. *Adv. Drug Deliv. Rev.* **64**, 18–23 (2012).
51. Yuk, H., Zhang, T., Parada, G. A., Liu, X. & Zhao, X. Skin-inspired hydrogel–elastomer hybrids with robust interfaces and functional microstructures. *Nat. Commun.* **7**, 12028 (2016).
52. Wirthl, D. et al. Instant tough bonding of hydrogels for soft machines and electronics. *Sci. Adv.* **3**, e1700053 (2017).
53. Liu, Q., Nian, G., Yang, C., Qu, S. & Suo, Z. Bonding dissimilar polymer networks in various manufacturing processes. *Nat. Commun.* **9**, 846 (2018).
54. Bai, Y. et al. Transparent hydrogel with enhanced water retention capacity by introducing highly hydratable salt. *Appl. Phys. Lett.* **105**, 151903 (2014).
55. Le Floch, P. et al. Wearable and washable conductors for active textiles. *ACS Appl. Mater. Interfaces* **9**, 25542–25552 (2017).
56. Tang, J., Li, J., Vlassak, J. J. & Suo, Z. Fatigue fracture of hydrogels. *Extreme Mechan. Lett.* **10**, 24–31 (2017).
57. Bai, R. et al. Fatigue fracture of tough hydrogels. *Extreme Mechan. Lett.* **15**, 91–96 (2017).
58. Zhang, W. et al. Fatigue of double-network hydrogels. *Eng. Fract. Mech.* **187**, 74–93 (2018).
59. Hu, X., Vatankhah-Varnoosfaderani, M., Zhou, J., Li, Q. & Sheiko, S. S. Weak hydrogen bonding enables hard, strong, tough, and elastic hydrogels. *Adv. Mater.* **27**, 6899–6905 (2015).
60. Yang, Y., Wang, X., Yang, F., Shen, H. & Wu, D. A universal soaking strategy to convert composite hydrogels into extremely tough and rapidly recoverable double-network hydrogels. *Adv. Mater.* **28**, 7178–7184 (2016).
61. Jeon, I., Cui, J., Illeperuma, W. R., Aizenberg, J. & Vlassak, J. J. Extremely stretchable and fast self-healing hydrogels. *Adv. Mater.* **28**, 4678–4683 (2016).
62. Haque, M. A., Kurokawa, T., Kamita, G. & Gong, J. P. Lamellar bilayers as reversible sacrificial bonds to toughen hydrogel: hysteresis, self-recovery, fatigue resistance, and crack blunting. *Macromolecules* **44**, 8916–8924 (2011).
63. Haque, M. A., Kurokawa, T. & Gong, J. P. Anisotropic hydrogel based on bilayers: color, strength, toughness, and fatigue resistance. *Soft Matter* **8**, 8008–8016 (2012).
64. Bai, T. et al. Construction of an ultrahigh strength hydrogel with excellent fatigue resistance based on strong dipole–dipole interaction. *Soft Matter* **7**, 2825–2831 (2011).
65. Du, G. et al. Tough and fatigue resistant biomimetic hydrogels of interlaced self-assembled conjugated polymer belts with a polyelectrolyte network. *Chem. Mater.* **26**, 3522–3529 (2014).
66. Lin, P., Ma, S., Wang, X. & Zhou, F. Molecularly engineered dual-crosslinked hydrogel with ultrahigh mechanical strength, toughness, and good self-recovery. *Adv. Mater.* **27**, 2054–2059 (2015).
67. Bai, R., Yang, J., Morelle, X. P., Yang, C. & Suo, Z. Fatigue fracture of self-recovery hydrogels. *ACS Macro Lett.* **7**, 312–317 (2018).
68. Dayan, P. & Abbott, L. F. *Theoretical Neuroscience*. Vol. 806 (MIT Press, Cambridge, MA, 2001).
69. Pelrine, R., Kornbluh, R., Pei, Q. & Joseph, J. High-speed electrically actuated elastomers with strain greater than 100%. *Science* **287**, 836–839 (2000).
70. Pelrine, R. E., Kornbluh, R. D. & Joseph, J. P. Electrostriction of polymer dielectrics with compliant electrodes as a means of actuation. *Sens. Actuators A Phys.* **64**, 77–85 (1998).
71. O'Halloran, A., O'malley, F. & McHugh, P. A review on dielectric elastomer actuators, technology, applications, and challenges. *J. Appl. Phys.* **104**, 9 (2008).
72. Carpi, F., De Rossi, D., Kornbluh, R., Pelrine, R. E. & Sommer-Larsen, P. *Dielectric Elastomers as Electromechanical Transducers: Fundamentals, Materials, Devices, Models and Applications of an Emerging Electroactive Polymer Technology*. (Elsevier, 2011).
73. Anderson, I. A., Gisby, T. A., McKay, T. G., O'Brien, B. M. & Calius, E. P. Multi-functional dielectric elastomer artificial muscles for soft and smart machines. *J. Appl. Phys.* **112**, 041101 (2012).
74. Brochu, P. & Pei, Q. Advances in dielectric elastomers for actuators and artificial muscles. *Macromol. Rapid Commun.* **31**, 10–36 (2010).
75. Suo, Z. Theory of dielectric elastomers. *Acta Mech. Solida Sin.* **23**, 549–578 (2010).
76. Zhao, X. & Wang, Q. Harnessing large deformation and instabilities of soft dielectrics: Theory, experiment, and application. *Appl. Phys. Rev.* **1**, 021304 (2014).
77. Poulin, A., Rosset, S. & Shea, H. R. Printing low-voltage dielectric elastomer actuators. *Appl. Phys. Lett.* **107**, 244104 (2015).
78. Duduta, M., Wood, R. J. & Clarke, D. R. Multilayer dielectric elastomers for fast, programmable actuation without prestretch. *Adv. Mater.* **28**, 8058–8063 (2016).
79. Madsen, F. B., Yu, L., Daugaard, A. E., Hvilsted, S. & Skov, A. L. Silicone elastomers with high dielectric permittivity and high dielectric breakdown strength based on dipolar copolymers. *Polymer* **55**, 6212–6219 (2014).
80. Zhang, Q. et al. An all-organic composite actuator material with a high dielectric constant. *Nature* **419**, 284 (2002).
81. Molberg, M. et al. High breakdown field dielectric elastomer actuators using encapsulated polyaniline as high dielectric constant filler. *Adv. Funct. Mater.* **20**, 3280–3291 (2010).
82. Madsen, F. B., Daugaard, A. E., Hvilsted, S. & Skov, A. L. The current state of silicone-based dielectric elastomer transducers. *Macromol. Rapid Commun.* **37**, 378–413 (2016).
83. Opris, D. M. Polar elastomers as novel materials for electromechanical actuator applications. *Adv. Mater.* **30**, 1703678 (2018).

84. Carpi, F., Frediani, G., Turco, S. & De Rossi, D. Bioinspired tunable lens with muscle-like electroactive elastomers. *Adv. Funct. Mater.* **21**, 4152–4158 (2011).
85. Rosset, S. & Shea, H. R. Flexible and stretchable electrodes for dielectric elastomer actuators. *Appl. Phys. A* **110**, 281–307 (2013).
86. Huang, J., Yang, J., Jin, L., Clarke, D. R. & Suo, Z. Pattern formation in plastic liquid films on elastomers by ratcheting. *Soft Matter* **12**, 3820–3827 (2016).
87. Morelle, X. P., Bai, R. & Suo, Z. Localized deformation in plastic liquids on elastomers. *J. Appl. Mech.* **84**, 101002 (2017).
88. McCoul, D., Hu, W., Gao, M., Mehta, V. & Pei, Q. Recent advances in stretchable and transparent electronic materials. *Adv. Electron. Mater.* **2**, 1500407 (2016).
89. Carpi, F., Chiarelli, P., Mazzoldi, A. & De Rossi, D. Electromechanical characterisation of dielectric elastomer planar actuators: comparative evaluation of different electrode materials and different counterloads. *Sens. Actuators A Phys.* **107**, 85–95 (2003).
90. Tavakol, B. & Holmes, D. P. Voltage-induced buckling of dielectric films using fluid electrodes. *Appl. Phys. Lett.* **108**, 112901 (2016).
91. Christianson, C., Goldberg, N., Cai, S. & Tolley, M. T. in *Electroactive Polymer Actuators and Devices (EAPAD) 2017* 101631O (Portland, OR, USA, 2017).
92. Bard, A. J. & Faulkner, L. R. Fundamentals and applications. *Electrochem. Methods* **2**, 482 (2001).
93. Rivnay, J. et al. Organic electrochemical transistors. *Nat. Rev. Mater.* **3**, 17086 (2018).
94. Hammock, M. L., Chortos, A., Tee, B. C. K., Tok, J. B. H. & Bao, Z. 25th anniversary article: the evolution of electronic skin (e-skin): a brief history, design considerations, and recent progress. *Adv. Mater.* **25**, 5997–6038 (2013).
95. Bauer, S. et al. 25th anniversary article: a soft future: from robots and sensor skin to energy harvesters. *Adv. Mater.* **26**, 149–162 (2014).
96. Rogers, J. A. Wearable electronics: nanomesh on-skin electronics. *Nat. Nanotechnol.* **12**, 839 (2017).
97. Lu, N. & Kim, D.-H. Flexible and stretchable electronics paving the way for soft robotics. *Soft Robot.* **1**, 53–62 (2014).
98. Manandhar, P., Calvert, P. D. & Buck, J. R. Elastomeric ionic hydrogel sensor for large strains. *IEEE Sens. J.* **12**, 2052–2061 (2012).
99. Tian, K. et al. 3D printing of transparent and conductive heterogeneous hydrogel–elastomer systems. *Adv. Mater.* **29**, 1604827 (2017).
100. Yuan-Hui, L. & Gregory, S. Diffusion of ions in sea water and in deep-sea sediments. *Geochim. Cosmochim. Acta* **38**, 703–714 (1974).
101. Bear, M. F., Connors, B. W. & Paradiso, M. A. *Neuroscience*. Vol. 2 (Lippincott Williams & Wilkins, 2007).
102. Robinson, S. S. et al. Integrated soft sensors and elastomeric actuators for tactile machines with kinesthetic sense. *Extreme Mechan. Lett.* **5**, 47–53 (2015).
103. Rogers, J. A., Someya, T. & Huang, Y. Materials and mechanics for stretchable electronics. *Science* **327**, 1603–1607 (2010).
104. Yang, S., Ng, E. & Lu, N. Indium Tin Oxide (ITO) serpentine ribbons on soft substrates stretched beyond 100%. *Extreme Mechan. Lett.* **2**, 37–45 (2015).
105. Na, S. I., Kim, S. S., Jo, J. & Kim, D. Y. Efficient and flexible ITO-free organic solar cells using highly conductive polymer anodes. *Adv. Mater.* **20**, 4061–4067 (2008).
106. Oh, J. Y. et al. Intrinsically stretchable and healable semiconducting polymer for organic transistors. *Nature* **539**, 411 (2016).
107. De Volder, M. F., Tawfick, S. H., Baughman, R. H. & Hart, A. J. Carbon nanotubes: present and future commercial applications. *Science* **339**, 535–539 (2013).
108. Sun, H., Zhang, Y., Zhang, J., Sun, X. & Peng, H. Energy harvesting and storage in 1D devices. *Nat. Rev. Mater.* **2**, 17023 (2017).
109. Liang, J., Li, L., Niu, X., Yu, Z. & Pei, Q. Elastomeric polymer light-emitting devices and displays. *Nat. Photon.* **7**, 817 (2013).
110. Langley, D. et al. Flexible transparent conductive materials based on silver nanowire networks: a review. *Nanotechnology* **24**, 452001 (2013).
111. Yoon, J. et al. Ultrathin silicon solar microcells for semitransparent, mechanically flexible and microconcentrator module designs. *Nat. Mater.* **7**, 907 (2008).
112. Lewis, J. Material challenge for flexible organic devices. *Mater. Today* **9**, 38–45 (2006).
113. Denisin, A. K. & Pruitt, B. L. Tuning the range of polyacrylamide gel stiffness for mechanobiology applications. *ACS Appl. Mater. Interfaces* **8**, 21893–21902 (2016).
114. Southan, A. et al. Toward controlling the formation, degradation behavior, and properties of hydrogels synthesized by Aza-Michael reactions. *Macromol. Chem. Phys.* **214**, 1865–1873 (2013).
115. Martini, M. et al. Charged triazole cross-linkers for hyaluronan-based hybrid hydrogels. *Materials* **9**, 810 (2016).
116. Gong, J. P., Katsuyama, Y., Kurokawa, T. & Osada, Y. Double-network hydrogels with extremely high mechanical strength. *Adv. Mater.* **15**, 1155–1158 (2003).
117. Sun, J.-Y. et al. Highly stretchable and tough hydrogels. *Nature* **489**, 133 (2012).
118. Kitai, A. *Luminescent Materials and Applications*. Vol. 25 (John Wiley & Sons, 2008).
119. Chopra, K. Dielectric properties of ZnS films. *J. Appl. Phys.* **36**, 655–656 (1965).
120. Hirabayashi, K., Kozawaguchi, H. & Tsujiyama, B. Study on A-C powder EL phosphor deterioration factors. *J. Electrochem. Soc.* **130**, 2259–2263 (1983).
121. Bender, J., Wager, J., Kissick, J., Clark, B. & Keszler, D. Zn2GeO4: Mn alternating-current thin-film electroluminescent devices. *J. Lumin.* **99**, 311–324 (2002).
122. Lee, J. S. et al. Robust moisture and thermally stable phosphor glass plate for highly unstable sulfide phosphors in high-power white light-emitting diodes. *Opt. Lett.* **38**, 3298–3300 (2013).
123. Xu, Q., Schmidt, B., Pradhan, S. & Lipson, M. Micrometre-scale silicon electro-optic modulator. *Nature* **435**, 325 (2005).
124. Yang, D.-K. *Fundamentals of Liquid Crystal Devices*. (John Wiley & Sons, 2014).
125. Kleman, M. & Laverntovich, O. D. *Soft Matter Physics: An Introduction*. (Springer Science & Business Media, 2007).
126. Sutherland, R., Tondiglia, V., Natarajan, L., Bunning, T. & Adams, W. Electrically switchable volume gratings in polymer-dispersed liquid crystals. *Appl. Phys. Lett.* **64**, 1074–1076 (1994).
127. Aguilar, R. & Meijer, G. in *Proceedings of IEEE Sensors, 2002* 1360–1363 (Orlando, FL, USA, 2002).
128. Krein, P. T. & Meadows, R. D. The electroquasistatics of the capacitive touch panel. *IEEE Trans. Ind. Appl.* **26**, 529–534 (1990).
129. Adler, R. & Desmares, P. J. An economical touch panel using SAW absorption. *IEEE Trans. Ultrason. Ferroelect., Freq. Control* **34**, 195–201 (1987).
130. Bhalla, M. R. & Bhalla, A. V. Comparative study of various touchscreen technologies. *IJCA* **6**, 12–18 (2010).
131. Tian, H. et al. A novel flexible capacitive touch pad based on graphene oxide film. *Nanoscale* **5**, 890–894 (2013).
132. Lai, Y. C. et al. Electric eel-skin-inspired mechanically durable and super-stretchable nanogenerator for deformable power source and fully autonomous conformable electronic-skin applications. *Adv. Mater.* **28**, 10024–10032 (2016).
133. Yi, F. et al. Stretchable and waterproof self-charging power system for harvesting energy from diverse deformation and powering wearable electronics. *ACS Nano* **10**, 6519–6525 (2016).
134. Niu, S. & Wang, Z. L. Theoretical systems of triboelectric nanogenerators. *Nano Energy* **14**, 161–192 (2015).
135. Gotter, A. L., Kaetzel, M. A. & Dedman, J. R. Electrophorus electricus as a model system for the study of membrane excitability. *Comp. Biochem. Physiol. A Mol. Integr. Physiol.* **119**, 225–241 (1998).
136. Xu, J. & Lavan, D. A. Designing artificial cells to harness the biological ion concentration gradient. *Nat. Nanotechnol.* **3**, 666 (2008).
137. Carpi, F., Frediani, G. & De Rossi, D. Hydrostatically coupled dielectric elastomer actuators. *IEEE/ASME Trans. Mechatron.* **15**, 308–315 (2010).
138. Pharr, M., Sun, J.-Y. & Suo, Z. Rupture of a highly stretchable acrylic dielectric elastomer. *J. Appl. Phys.* **111**, 104114 (2012).
139. Chen, C., Wang, Z. & Suo, Z. Flaw sensitivity of highly stretchable materials. *Extreme Mechan. Lett.* **10**, 50–57 (2017).
140. Gong, J. P. Why are double network hydrogels so tough? *Soft Matter* **6**, 2583–2590 (2010).
141. Peak, C. W., Wilker, J. J. & Schmidt, G. A review on tough and sticky hydrogels. *Colloid. Polym. Sci.* **291**, 2031–2047 (2013).
142. Zhao, X. Multi-scale multi-mechanism design of tough hydrogels: building dissipation into stretchy networks. *Soft Matter* **10**, 672–687 (2014).
143. Long, R. & Hui, C.-Y. Crack tip fields in soft elastic solids subjected to large quasi-static deformation — a review. *Extreme Mechan. Lett.* **4**, 131–155 (2015).
144. Creton, C. 50th anniversary perspective: networks and gels: soft but dynamic and tough. *Macromolecules* **50**, 8297–8316 (2017).
145. Wang, W., Zhang, Y. & Liu, W. Bioinspired fabrication of high strength hydrogels from non-covalent interactions. *Prog. Polym. Sci.* **71**, 1–25 (2017).
146. Zhang, Y. S. & Khademhosseini, A. Advances in engineering hydrogels. *Science* **356**, eaaf3627 (2017).
147. Buwalda, S. J. et al. Hydrogels in a historical perspective: from simple networks to smart materials. *J. Control. Release* **190**, 254–273 (2014).
148. Griffith, A. The phenomena of flow and rupture in solids. *Philos. Trans. R. Soc. A* **221**, 163–198 (1920).
149. Lake, G. & Thomas, A. The strength of highly elastic materials. *Proc. R. Soc. Lond. A* **300**, 108–119 (1967).
150. Andrews, E. Rupture propagation in hysteresial materials: stress at a notch. *J. Mech. Phys. Solids* **11**, 231–242 (1963).
151. Evans, A. G. Perspective on the development of high-toughness ceramics. *J. Am. Ceram. Soc.* **73**, 187–206 (1990).
152. Tvergaard, V. & Hutchinson, J. W. The relation between crack growth resistance and fracture process parameters in elastic-plastic solids. *J. Mech. Phys. Solids* **40**, 1377–1397 (1992).
153. Bao, G. & Suo, Z. Remarks on crack-bridging concepts. *Appl. Mech. Rev.* **45**, 355–366 (1992).
154. Du, J., Thouless, M. & Yee, A. Effects of rate on crack growth in a rubber-modified epoxy. *Acta Mater.* **48**, 3581–3592 (2000).
155. Ducrot, E., Chen, Y., Bulters, M., Sijbesma, R. P. & Creton, C. Toughening elastomers with sacrificial bonds and watching them break. *Science* **344**, 186–189 (2014).
156. Tang, J., Li, J., Vlassak, J. J. & Suo, Z. Adhesion between highly stretchable materials. *Soft Matter* **12**, 1093–1099 (2016).
157. Yuk, H., Zhang, T., Lin, S., Parada, G. A. & Zhao, X. Tough bonding of hydrogels to diverse non-porous surfaces. *Nat. Mater.* **15**, 190 (2016).
158. Li, J. et al. Tough adhesives for diverse wet surfaces. *Science* **357**, 378–381 (2017).
159. Ebnesajjad, S. & Landrock, A. H. *Adhesives Technology Handbook* (William Andrew, 2014).
160. Yang, J., Bai, R. & Suo, Z. Topological adhesion of wet materials. *Adv. Mater*. https://doi.org/10.1002/adma.201800671 (2018).
161. Efimenko, K., Wallace, W. E. & Genzer, J. Surface modification of Sylgard-184 poly (dimethyl siloxane) networks by ultraviolet and ultraviolet/ozone treatment. *J. Colloid Interface Sci.* **254**, 306–315 (2002).
162. Hegemann, D., Brunner, H. & Oehr, C. Plasma treatment of polymers for surface and adhesion improvement. *Nucl. Instrum. Methods Phys. Res. B* **208**, 281–286 (2003).
163. Bodas, D. & Khan-Malek, C. Hydrophilization and hydrophobic recovery of PDMS by oxygen plasma and chemical treatment — an SEM investigation. *Sens. Actuators B* **123**, 368–373 (2007).
164. Dissado, L. A. & Fothergill, J. C. *Electrical Degradation and Breakdown in Polymers*. Vol. 9 (IET, 1992).
165. Barry, R. A. et al. Direct-write assembly of 3D hydrogel scaffolds for guided cell growth. *Adv. Mater.* **21**, 2407–2410 (2009).
166. Levinson, P., Cazabat, A., Stuart, M. C., Heslot, F. & Nicolet, S. The spreading of macroscopic droplets. *Rev. Phys. Appl.* **23**, 1009–1016 (1988).
167. Wu, H. et al. Transfer printing of metallic microstructures on adhesion-promoting hydrogel substrates. *Adv. Mater.* **27**, 3398–3404 (2015).
168. Kusaka, I. & Suëtaka, W. Infrared spectrum of α-cyanoacrylate adhesive in the first monolayer on a bulk aluminum surface. *Spectrochim. Acta A* **36**, 647–648 (1980).
169. Schneider, M. H., Tran, Y. & Tabeling, P. Benzophenone absorption and diffusion in poly (dimethylsiloxane) and its role in graft photo-polymerization for surface modification. *Langmuir* **27**, 1232–1240 (2011).

170. Wang, Y. et al. Covalent micropatterning of poly (dimethylsiloxane) by photografting through a mask. *Anal. Chem.* **77**, 7539–7546 (2005).
171. Simmons, C. S., Ribeiro, A. J. & Pruitt, B. L. Formation of composite polyacrylamide and silicone substrates for independent control of stiffness and strain. *Lab Chip* **13**, 646–649 (2013).
172. Rose, S. et al. Nanoparticle solutions as adhesives for gels and biological tissues. *Nature* **505**, 382 (2014).
173. Young, J. F. Humidity control in the laboratory using salt solutions — a review. *J. Chem. Technol. Biotechnol.* **17**, 241–245 (1967).
174. Root, S. E. et al. Ionotactile stimulation: nonvolatile ionic gels for human–machine interfaces. *ACS Omega* **3**, 662–666 (2018).
175. Chen, B. et al. Highly stretchable and transparent ionogels as nonvolatile conductors for dielectric elastomer transducers. *ACS Appl. Mater. Interfaces* **6**, 7840–7845 (2014).
176. Le Bideau, J., Viau, L. & Vioux, A. Ionogels, ionic liquid based hybrid materials. *Chem. Soc. Rev.* **40**, 907–925 (2011).
177. Suresh, S. *Fatigue of Materials* (Cambridge Univ Press, 1998).
178. Ritchie, R. O. Mechanisms of fatigue-crack propagation in ductile and brittle solids. *Int. J. Fracture* **100**, 55–83 (1999).
179. Li, J., Suo, Z. & Vlassak, J. J. Stiff, strong, and tough hydrogels with good chemical stability. *J. Mater. Chem. B* **2**, 6708–6713 (2014).
180. Sun, T. L. et al. Physical hydrogels composed of polyampholytes demonstrate high toughness and viscoelasticity. *Nat. Mater.* **12**, 932 (2013).
181. Lin, S. et al. Stretchable hydrogel electronics and devices. *Adv. Mater.* **28**, 4497–4505 (2016).
182. Wu, H. et al. Stable Li-ion battery anodes by in-situ polymerization of conducting hydrogel to conformally coat silicon nanoparticles. *Nat. Commun.* **4**, 1943 (2013).
183. Guiseppi-Elie, A. Electroconductive hydrogels: synthesis, characterization and biomedical applications. *Biomaterials* **31**, 2701–2716 (2010).
184. Cheong, G. M. et al. Conductive hydrogels with tailored bioactivity for implantable electrode coatings. *Acta Biomaterialia* **10**, 1216–1226 (2014).
185. Overvelde, J. T. et al. Mechanical and electrical numerical analysis of soft liquid-embedded deformation sensors analysis. *Extreme Mechan. Lett.* **1**, 42–46 (2014).
186. Alirezaei, H., Nagakubo, A. & Kuniyoshi, Y. in *2007 7th IEEE-RAS International Conference on Humanoid Robots* 167–173 (Pittsburgh, PA, USA, 2007).
187. Hong, S. et al. 3D printing of highly stretchable and tough hydrogels into complex, cellularized structures. *Adv. Mater.* **27**, 4035–4040 (2015).
188. Truby, R. L. et al. Soft somatosensitive actuators via embedded 3D printing. *Adv. Mater*. https://doi.org/10.1002/adma.201706383 (2018).
189. Frutiger, A. et al. Capacitive soft strain sensors via multicore–shell fiber printing. *Adv. Mater.* **27**, 2440–2446 (2015).
190. Xiong, W. et al. Highly conductive, air-stable silver nanowire@iongel composite films toward flexible transparent electrodes. *Adv. Mater.* **28**, 7167–7172 (2016).
191. Kim, D., Lee, G., Kim, D. & Ha, J. S. Air-stable, high-performance, flexible microsupercapacitor with patterned ionogel electrolyte. *ACS Appl. Mater. Interfaces* **7**, 4608–4615 (2015).
192. Zhang, S., Wang, F., Peng, H., Yan, J. & Pan, G. Flexible highly sensitive pressure sensor based on ionic liquid gel film. *ACS Omega* **3**, 3014–3021 (2018).
193. Kamio, E., Yasui, T., Iida, Y., Gong, J. P. & Matsuyama, H. Inorganic/organic double-network gels containing ionic liquids. *Adv. Mater.* **29**, 1704118 (2017).
194. Chen, N., Zhang, H., Li, L., Chen, R. & Guo, S. Ionogel electrolytes for high-performance lithium batteries: a review. *Adv. Energy Mater*. https://doi.org/10.1002/aenm.201702675 (2018).

Acknowledgements
The authors acknowledge financial support from the National Science Foundation Materials Research Science and Engineering Centers (DMR-1420570). The authors thank collaborators at Harvard University and Xi'an Jiaotong University for much of the work reviewed here. In particular, the co-authors of reference 21, C. Keplinger, J.-Y. Sun, C. C. Foo, P. Rothemund and G. Whitesides, helped shape a long view of hydrogel ionotronics.

Author contributions
All authors contributed equally to the preparation of this manuscript.

Competing interests
The authors declare no competing interests.

Publisher's note
Springer Nature remains neutral with regard to jurisdictional claims in published maps and institutional affiliations.